Synthesis of a Multichromophoric Array by Sequential CuAAC Reactions

Assia Tafrioucht, Jad Rabah, Krystyna Baczko, Hélène Fensterbank, Rachel Méallet-Renault, Gilles Clavier, François Couty, Emmanuel Allard, Karen Wright

Synthesis of a Multichromophoric Array by Sequential CuAAC Reactions

Assia Tafrioucht,[a] Jad Rabah,[a] Krystyna Baczko,[a] Hélène Fensterbank,[a] Rachel Méallet-Renault,[b] Gilles Clavier,[c] François Couty,[a] Emmanuel Allard,[a] Karen Wright[a*]

An easily synthesized α-hydroxy-β-azidotetrazole scaffold was used to build a three dimensional polychromic system. Different chromophores (coumarin, BODIPY and distyryl BODIPY) were incorporated into the structure by using sequential CuAAC reactions to form a series of dyads and a triad. A computational study of the resulting arrays showed that the predominant conformations brought the substituents into close spatial proximity. The triad exhibited FRET behaviour with notably efficient energy transfer values.

a Université Paris-Saclay, UVSQ, CNRS, UMR 8180, Institut Lavoisier de Versailles, 78000, Versailles, France

b Université Paris-Saclay, CNRS, Institut des Sciences Moléculaires d'Orsay, 91405, Orsay, France.

c Université Paris-Saclay, ENS Paris-Saclay, CNRS, Photophysique et Photochimie Supramoléculaires et Macromoléculaires, 91190 Gif-sur-Yvette, France.

Keywords: Fluorescence**,** Synthesis**,** Electronic energy transfer, BODIPY chromophores

1. Introduction

Multifunctional chemical scaffolds which can be orthogonally substituted with varied chemical groups represent important tools in the fields of chemistry and biology.[1,2] From a relatively simple basic structure, complex chemical architectures can be created from such scaffolds in only a few steps, by using successive coupling reactions to associate diverse molecules, such as peptides, nucleotides, carbohydrates or fluorophores. “Click” reactions, which should be high-yielding and regiospecific, are ideal for use in this context.[3-7] The

copper-catalyzed azide–alkyne cycloaddition (CuAAC) reaction has become the most popular of these reactions, as it is compatible with varied functional groups and requires only mild reaction conditions.[8-10]

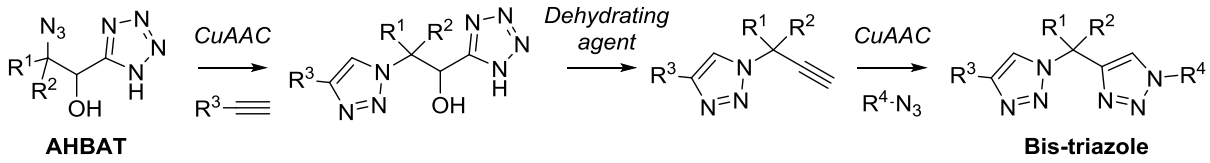

Scheme 1. Bis-triazole synthesis from α-hydroxy-β-azidotetrazoles (AHBATs).

We recently reported the use of α-hydroxy-β-azidotetrazoles (AHBATs) as substrates for orthogonal CuAAC reactions.[11] These compounds are easily prepared from α,β-epoxynitriles by tin-catalyzed cycloaddition and ring opening with $TMSN_3$.[12] The azide moiety of these molecules may undergo a first CuAAC reaction with an alkyne, and the α-hydroxytetrazole part subsequently converted to an alkyne by treatment with a dehydrating agent (scheme 1).[12,13] This alkyne can then react with an azide in a second CuAAC reaction, leading to unsymmetrical bis-triazoles. This synthetic strategy was found to be compatible with a range of functional groups, and could be used to create structural diversity around the central carbon atom.

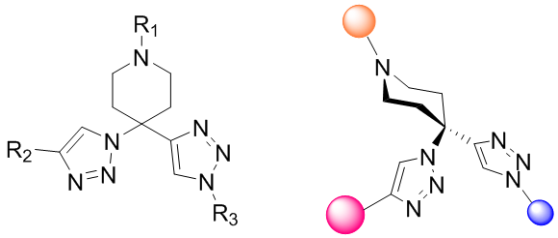

Figure 1. Tri-functionalised piperidine-bis-triazole scaffold

The previously described AHBATs constitute a bifunctional scaffold, but we reasoned that additional orthogonal attachment points could be created by introducing suitable reactive moieties at the central carbon atom (groups R^1/R^2 in Scheme 1) leading to a multifunctional platform, with the substituents placed in a three dimensional arrangement. We considered the use of a piperidine moiety in the AHBAT scaffold, giving an additional orthogonal attachment point, leading to a platform which could bear three different functional groups (figure 1). To demonstrate the possibilities of such a scaffold, we decided to functionalize this platform with three different chromophores, giving rise to a multichromophoric array.

Multichromophoric species have been extensively investigated in the last decade.[14-16] These assemblies, where chromophores are associated in covalently linked architectures, are able to harvest sunlight over a broad range of wavelengths, and subsequently concentrate photons at a preferred site by multiple electronic (or excitation) energy transfer (EET) processes. These properties are exploited for energy conversion in artificial photosynthesis and in solar cells.[15, 17-22] Moreover, multichromophoric species featuring EET properties are also sought for biomedical applications.[23,24] In addition, assemblies based on host-guest strategies have also led to efficient light harvesting materials.[25-28]

Numerous multichromophoric organic architectures with different combinations of chromophores have been described. Among the different chromophores, BODIPY dyes and their derivatives are of particular interest since they display high absorption coefficients, high fluorescent quantum yields and good photostability.[29-33] More importantly, the BODIPY core is easily functionalized, allowing tuning of absorption and emission properties, from the visible to the near infra-red region. Multi-BODIPY systems have been described using various pre-organized platforms, [19,20] and the geometry of these scaffolds used to associate the chromophores has a direct influence on the outcome of EET processes. At the most simple level, BODIPY dyes can be directly linked together, or connected through the use of a saturated or unsaturated spacer, leading to basically linear systems.[27,34-39] Two-dimensional systems, where the chromophores are arranged in a plane, can be formed from truxene scaffolds or by using a flat scaffold (including BODIPY) as a central core connecting

to several others.[40-43] Three-dimensional systems are more scarce, a few examples have been described using supports such as polymers,[44,45] carbohydrates,[46] dendrimers,[47,48] fullerene,[49] rotaxane[50] and triptycene derivatives.[51-53] In this latter approach, the non-planar spatial arrangement of the multichromophoric arrays may prevent aggregation of the chromophores. However, as the complexity of these scaffolds increases, the need for lengthy synthetic pathways or the limited possibilities to combine different chromophores may become drawbacks.

In this work, we propose to use our AHBAT modified platform with its tetrahedral architecture for the construction of multichromophoric systems. This platform, featuring three different functional groups (piperidine, azide and masked alkyne) with their distinct chemical reactivities, permits the grafting of individual chromophores in an efficient manner. We chose to use as fluorophores 7-diethylaminocoumarin, BODIPY and distyrylBODIPY for their complementary absorptions, that cover the entire visible spectral range. Adequate spectral overlap between the fluorescence donor emission and the acceptor absorption of each pair of chromophores was also considered in this study. The coumarin derivative (**Coum**) was selected as the short-wavelength donor due to its strong absorption and intense fluorescence in the blue spectral region.[54] The BODIPY dye, (**BDP**), chosen on the basis of its strong absorption and emission in the green region,[55] behaves both as donor and acceptor. Finally, the distyrylBODIPY (**DSBDP**, acceptor moiety) was selected due to its strong and highly efficient emission in the red/NIR spectral region.[56] The association of a coumarin donor with a BODIPY acceptor within an array has previously been investigated, notably for applications as laser dyes,[57] as artificial photosynthetic systems,[58] and for analyte detection in living cells.[59-61] Here we describe the synthesis and characterization of three dyads and a triad containing these three chromophores on the same platform. Absorption spectra and photophysical experiments were first conducted on the three dyads to characterise the energy transfer between each pair of chromophores. Finally, the same set of

experiments was carried out on the **Coum-BDP-DSBDP** triad to elucidate the overall EET process in this multichromophoric system.

2. Results and Discussion

2.1 Synthesis.

To create the desired tri-functional platform, an AHBAT with an additional, orthogonal attachment point was required. This scaffold could be synthesized in two experimentally simple, high yielding steps from commercial Boc-piperidone using our previously described procedure (cyano-epoxide formation, then $TMSN_3$ addition) to give the piperidine derived AHBAT **2**.[62] While the base resistant Boc protecting group was suitable for the synthesis of the AHBAT, the acidic conditions required for its later removal are incompatible with BODIPY chromophores,[63] so at this point it was replaced either with a Fmoc group (**3**), or with an *N*-diethyl coumarin fluorophore (**8**). The **BDP-DSBDP** dyad **7** was derived from the Fmoc protected AHBAT **3**, **BDP-alkyne** [64] and **DSBDP-N_3** using a three step CuAAC-alkyne formation-CuAAC strategy (Scheme 2). The CuAAC reactions were performed with copper sulphate/sodium ascorbate as the Cu(I) source, in the presence of TBTA as ligand [65] and were generally high-yielding. Alkyne formation was carried out by treating the intermediate triazole hydroxy-tetrazole with EDC in dichloromethane. The **Coum-DSBDP** dyad **11** and **Coum-BDP** dyad **13**, and the **Coum-BDP-DSBDP** triad **14** were all derived from **8** by using a similar strategy, as described in Scheme 3.

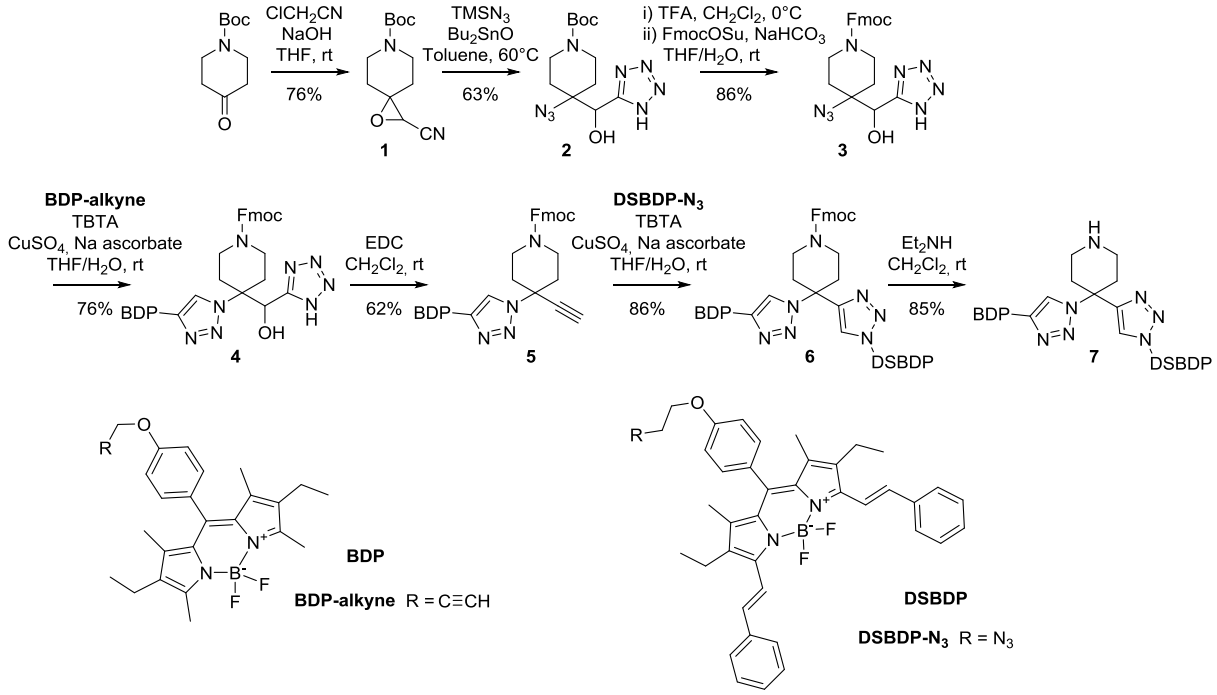

Scheme 2. Synthesis of the **BDP-DSBDP** dyad **7**.

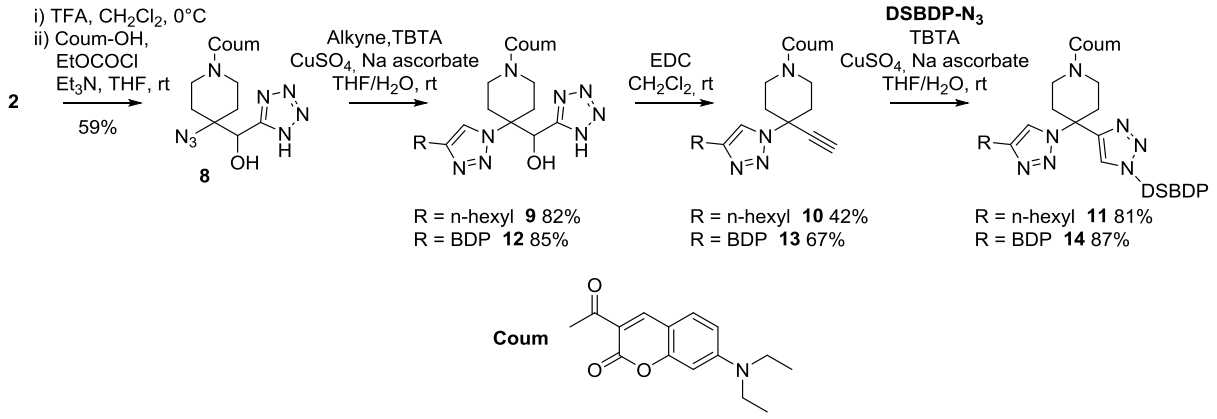

Scheme 3. Synthesis of the **Coum-DSBDP** and **Coum-BDP** dyads **11** and **13**, and the **Coum-BDP-DSBDP** triad **14**.

2.2 Computational studies

In order to define the three-dimensional spatial arrangement of the chromophores within this system, computational studies were performed on the dyads and triad. The conformational search of the molecular dyads (**BDP-DSBDP 7, Coum-DSBDP 11, Coum-BDP 13**) was carried out by theoretical calculations at the PM3 semi-empirical level using the Gaussian 09 program.[66] Owing to the very large number of degrees of freedom in these dyads, a full analysis of the potential energy surfaces (PES) would be too time consuming. Thus, a simplified strategy has been preferred by studying three fragments of the dyads (Figure S1). The PES of these fragments were first scanned around their relevant degrees of freedom (dihedral angles centred on the bonds marked in red – see supporting information) to find their most stable conformers, which were then used as initials points for geometrical optimizations of the dyads.

The phenyl-triazole (1st fragment) was first optimized by performing relaxed scans around its most flexible bonds (in red, Figure S1a), separately. The potential energy diagrams of each scan around the corresponding dihedral angles are presented in the supporting information (Figures S2-S4). Then, unconstrained geometry optimizations of the phenyl-triazole were carried out by starting from selected structures of the scan corresponding to the constrained minima. Three stable conformers were obtained from these optimizations (Figure 2a)

Next optimization of the second fragment (obtained by adding a second phenyl-triazole to the lower energy structure of the first fragment) was performed. The conformational search (Figure S5-S7) of this new fragment was performed firstly by a relaxed scan around the three flexible bonds (in red) of the added phenyl-triazole (black, Figure S1b). As previously, unconstrained geometry optimizations of the di(phenyl-triazole) was then performed starting from the constrained minima. Three remarkable conformers were obtained, the most stable adopting a structure in which the two phenyls rings are pointing upwards. In the other two, the two phenyl rings are pointing in opposite directions, upwards and downwards (Figure 2b).

The conformational search of the third fragment, which was obtained by adding the coumarin residue to the most stable conformer of the second fragment, was finally performed. This analysis was firstly done by a relaxed scan around the two most flexible bonds (red) of the coumarin-piperidine link (black, Figure S1c). Unconstrained optimizations of the di(phenyl-triazole)-coumarin were then made by starting from the constrained minima, which led to two stable conformers (Figure 2c).

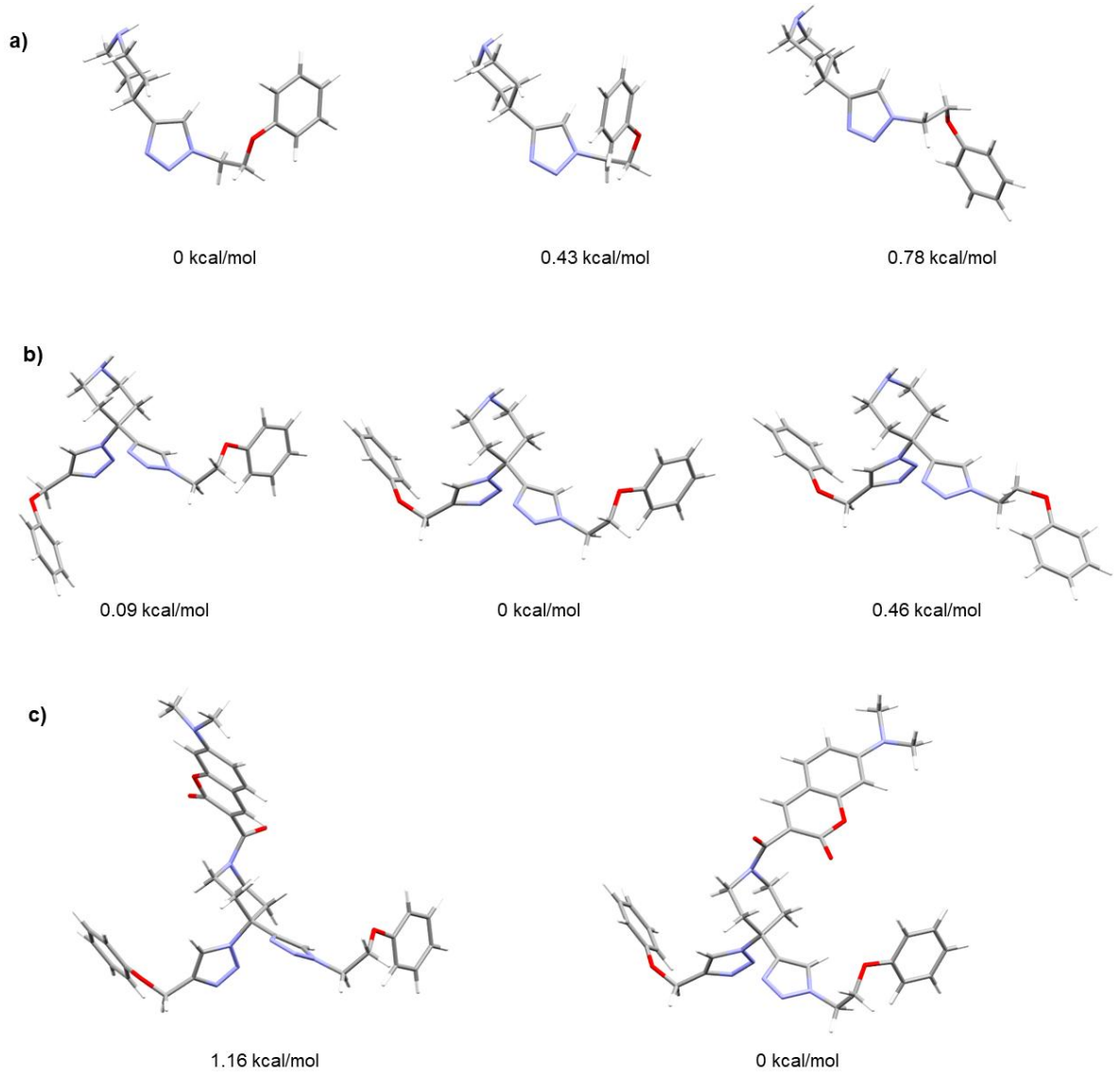

Figure 2. Most stable conformers of the three fragments with their relative energies: (a) phenyl-triazole, (b) di(phenyl-triazole) and (c) di(phenyl-triazole)-coumarin.

The final stage of this computational study was dedicated to the geometrical optimization of the dyads (**BDP-DSBDP 7, Coum-DSBDP 11, Coum-BDP 13**) and the triad (**Coum-BDP-DSBDP 14**). This analysis was performed starting from the minima obtained for the two fragments (di(phenyl-triazole) and di(phenyl-triazole)-coumarin along with the BODIPY and distyrylBODIPY chromophores. In addition, we also considered at least one of the other remarkable conformers of these fragments (Figure S10). The most stable conformers obtained for the dyads are presented in Figure 3. From this conformational analysis, the center-to-center distances between the chromophores in the dyads were also determined. For the **BDP-DSBDP** dyad **7**, the two BODIPY are pointing upwards, with a BODIPY-distyrylBODIPY distance of 18.2 Å. For the **Coum-DSBDP** and **Coum-BDP** dyads **11** and **13**, the chromophoric units are closer, with a coumarin-DistyrylBODIPY distance of 9.1 Å and a coumarin-BODIPY distance of 13.7 Å. We can note that the conformer of the **Coum-DSBDP** dyad is rather strained, with the two chromophores being very close to each other. The geometrical optimization starting from the other remarkable conformer of di(phenyl-triazole)-coumarin led to a conformer higher in energy (5.8 kcal/mol), in which the Coumarin and the distyrylBODIPY are pointing in opposite directions (Figure S12).

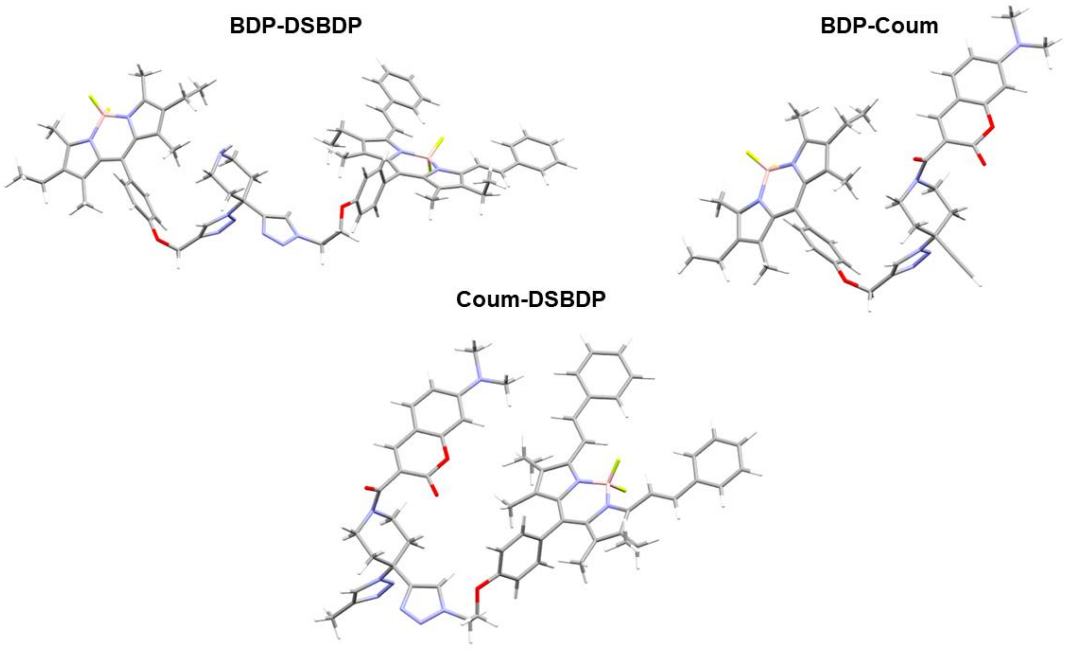

Figure 3. Representation of the most stable conformers of the dyads: BODIPY-distyrylBODIPY (**BDP-DSBDP 7**), BODIPY-coumarin (**Coum-BDP 13**) and coumarin-distyrylBODIPY (**Coum-DSBDP 11**). For the computational study, the phenyltriazole was replaced by an alkynyl group in the **Coum-BDP** dyad and the methoxyphenyl group was substituted for a methyl group in the **Coum-DSBDP** dyad.

Finally, geometrical optimization of the triad was performed using the results obtained from the studies of the fragments and dyads. This geometrical optimization gave at least two conformers, denoted as conformer I and II (Figure 4). Conformer I adopts a conformation in which the three chromophoric units are located in a confined area, and are pointing upwards. In conformer II the three chromophoric units are spread out, pointing in different directions. This conformer is higher in energy than conformer I by 6.7 kcal/mol.

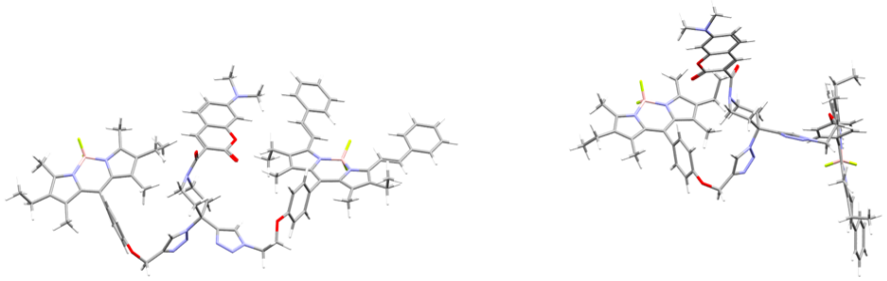

Figure 4. Representation of the most stable conformers of the triad **Coum-BDP-DSBDP 14** with their relative energies

A single point energy calculation was done on the most stable conformers of the dyads at the b3lyp/6-31+g(d,p) level and frontier molecular orbitals (MO) plotted (figure 5). In all cases, the MOs are located on each chromophoric moiety without delocalization. Furthermore the HOMO (abbreviated as HO) and LUMO (abbreviated as LU) are always centred on the chromophore that absorbs light at the lowest energy while the HOMO-1 (HO-1) and LUMO+1 (LU+1) are located on the chromophore that absorbs light at the highest energy. It can thus be concluded that in the dyads, the chromophores are independent in the ground state.

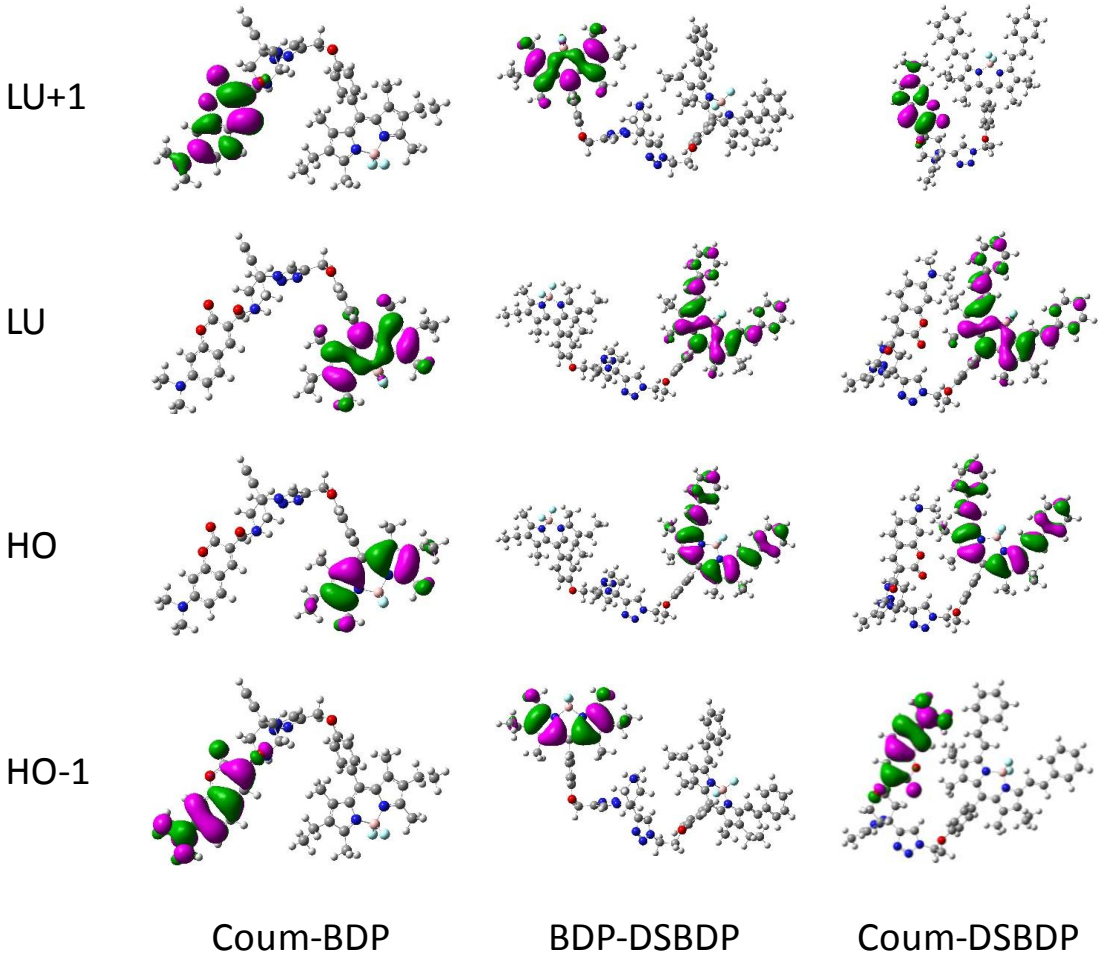

Figure 5. Plot of the frontier molecular orbitals of the 3 dyads **Coum-BDP 13**, **BDP-DSBDP 7** and **Coum-DSBDP 11** (isovalue 0.02)

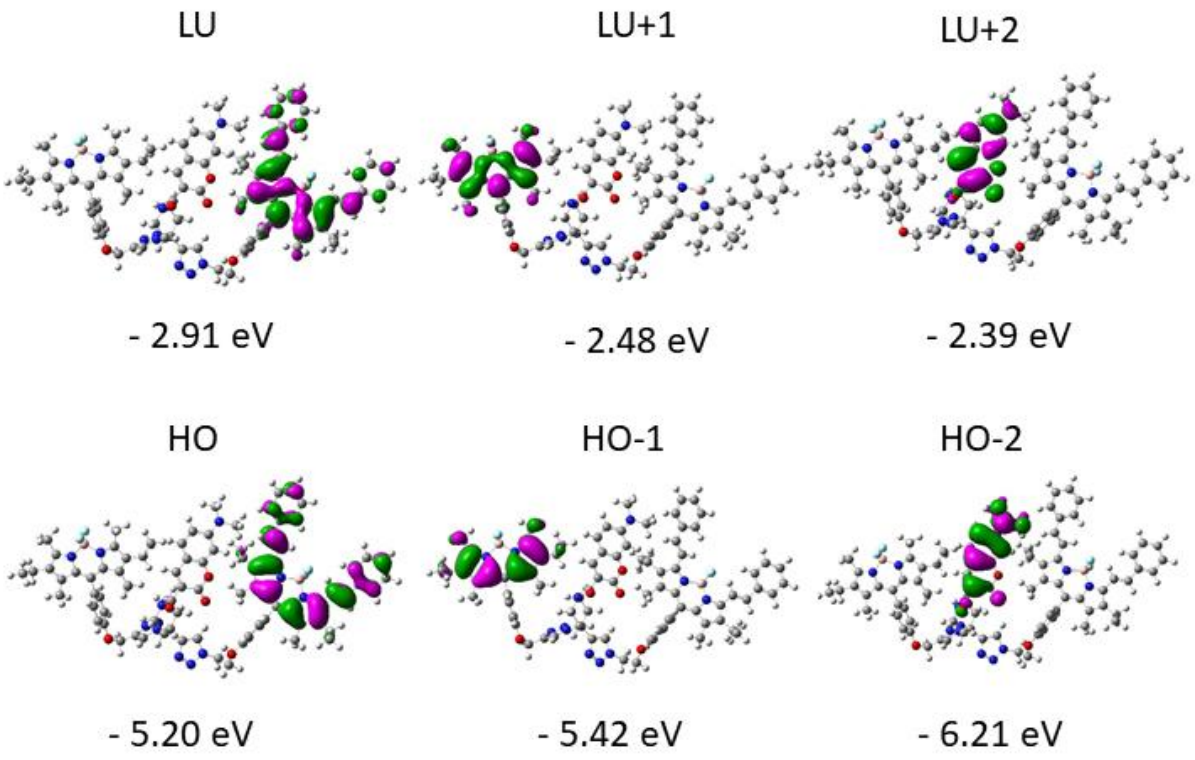

Figure 6. Plot of the frontier molecular orbitals of the triad-**conformer I Coum-BDP-DSBDP 14** (isovalue 0.02) with their energies in eV.

In addition, a single point energy calculation was also performed on the triad using the same level of theory as the dyads (figure 6). As pointed out earlier, MO are localized on the coumarin or BODIPY or distyrylBODIPY parts, indicating that the chromophores within the triad are independent in the ground state.

2.3 UV-vis absorption and fluorescence spectroscopy

Table 1. Absorption and emission properties of the dyads, triad and parent chromophores in dichloromethane.

Compound	λ_{abs} [nm] (log ε)	λ_{em} [nm]	ϕ_f [a]
Coum (**10**)	405 (4.38)	446[b]	0.84[b]
BDP-alkyne	370 (3.92), 525 (4.78)	536[c]	0.91[c]
DSBDP-N_3	345 (4.87), 636 (4.88)	651[d]	0.91[d]
Coum-BDP (**13**)	403 (4.53), 525 (4.79)	537[b]	0.023[b, e] 0.70[c, f]
Coum-DSBDP (**11**)	346 (4.85), 405 (4.53), 636 (4.84)	652[b]	0.0143[b, e] 0.40[d, g]
BDP-DSBDP (**7**)	346 (4.82), 526 (4.77), 637 (4.81)	654[c]	0.0156[c, h] 0.71[d, g]
Coum-BDP-DSBDP (**14**)	346 (4.96), 403 (4.67), 526 (4.88), 637 (4.93)	653[b] 654[c]	0.00678[b, e] 0.011[c, h] 0.45[d, g]

[a] ϕ_f is the relative fluorescence quantum yield estimated by using quinine sulfate (ϕ_f = 0.546 in 0.5M H_2SO_4) for **Coum** (**10**), rhodamine 6G (ϕ_f = 0.95 in EtOH) for **BDP-alkyne**, or oxazine 1 (ϕ_f = 0.11 in MeOH) for **DSBDP-N_3** as the fluorescence reference standards. [b] Excited at 400 nm. [c] Excited at 495 nm. [d] Excited at 605 nm. [e] Due to the donor (**Coum**) part. [f] Due to the acceptor (**BDP**) part. [g] Due to the acceptor (**DSBDP**) part. [h] Due to the donor (**BDP**) part.

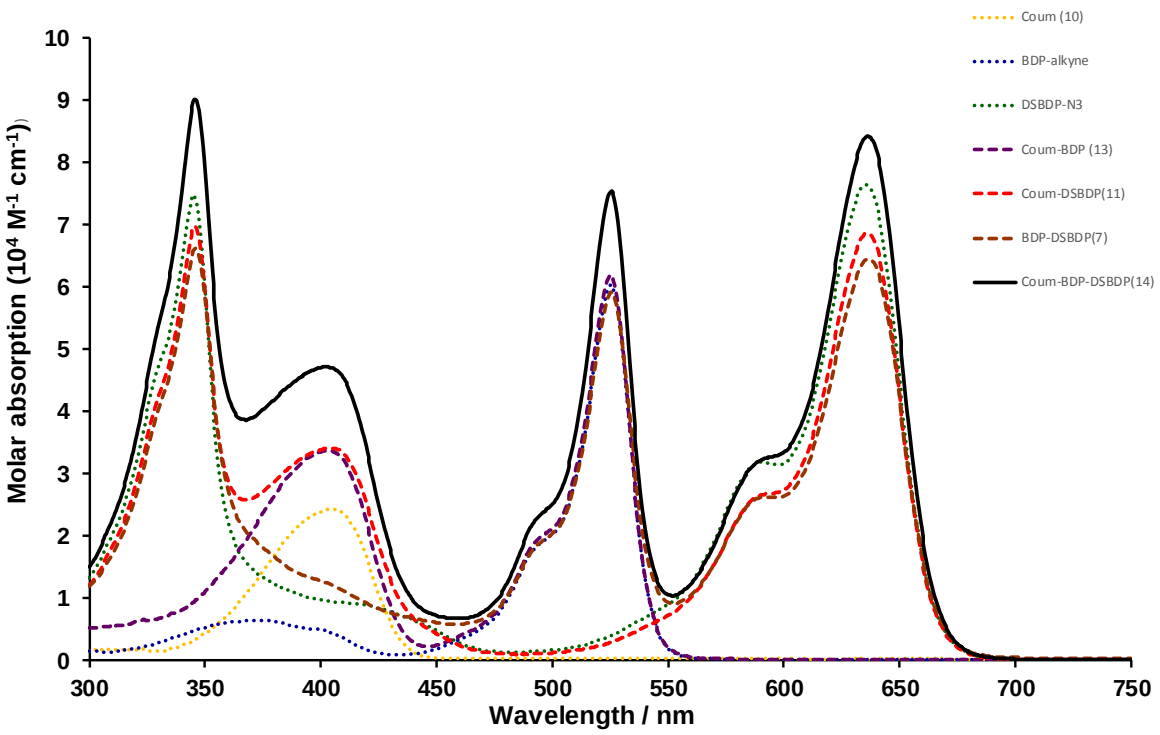

Figure 7. Absorption spectra of molecular triad (**Coum-BDP-DSBDP 14**), molecular dyads (**BDP-DSBDP 7, Coum-DSBDP 11, Coum-BDP 13**), and parent chromophores coumarin (**Coum 10**), BODIPY (**BDP-alkyne**) and distyrylBODIPY (**DSBDP-N_3**) in dichloromethane.

Figures 7 shows the absorption spectra of the molecular triad (**Coum-BDP-DSBDP 14**) and molecular dyads (**BDP-DSBDP 7, Coum-DSBDP 11, Coum-BDP 13**), as well as the spectra of the parent chromophores coumarin (**10**), BODIPY (**BDP-alkyne**) and distyrylBODIPY (**DSBDP-N_3**). The coumarin parent chromophore exhibited an absorption in the blue region located at 405 nm. The spectrum of the BODIPY showed a strong S_o->S_1 transition at 525 nm and a small S_o->S_2 transition at 371 nm, while the spectrum of the distyrylBODIPY exhibited a strong S_o->S_1 transition at 636 nm, red-shifted compared to that of BODIPY. The additional bands in the UV region are ascribed to the π-π* transitions of the distyryl subunits (345 nm) along with a shoulder attributed to the S_o->S_2 transition of the BODIPY backbone. The triad **14** containing the three parent chromophores showed the absorption characteristic maxima of coumarin, BODIPY and distyrylBODIPY with no significant spectral shifts or bandshape changes. This finding indicates that the

chromophores in the triad do not have significant ground state interactions. The same observation can be made for the dyads containing two of the three parent chromophores, which is consistent with the frontier molecular orbital discussion above. The fluorescence spectra of the parent chromophores were also recorded (Figures S22-S24). The coumarin **10**, BODIPY (**BDP-alkyne**) and distryrylBODIPY (**DSBDP-N_3**) derivatives exhibited strong fluorescence at 446 nm (λ_{exc}=400 nm), 536 nm (λ_{exc}=495 nm) and 651 nm (λ_{exc}=605 nm), respectively. Luminescence quantum yields can be found in Table 1. The spectroscopic characteristics of the parent molecules are fully consistent with those expected for these dyes. In the dyads and triad, the donor moiety was strongly quenched, indicating that an energy transfer is likely to occur. The absorption and emission spectra of the dyads and triad were also recorded in other solvents (methanol, acetonitrile and toluene, figures S14-21, table S1). Slight hypsochromic shifts were observed in the spectra of the dyads and triad containing the BODIPY entities with increasing solvent polarity, as has been previously observed.[67]

2.4 FRET Studies

In order to decipher the energy transfer processes in the triad, we firstly studied the fluorescence properties of three dyads containing two of the three parent chromophores. Excitation energy transfer (EET) can take place via two pathways: through-bond energy transfer (TBET) and fluorescence resonance energy transfer (FRET) [68]. The former (Dexter mechanism) can be excluded since the strong orbital overlap that is required between the donor and acceptor species is not satisfied in our systems. For the Förster mechanism, the efficiency of energy transfer is primarily controlled by three parameters: (1) the spectral overlap between the energy donor (D) emission and the energy acceptor (A) absorption; (2) the distance between the donor and the acceptor; (3) the relative orientation of the electronic transition dipole moments of the donor (D) and acceptor (A). The coumarin-BODIPY **Coum-BDP 13**, coumarin-distyrylBODIPY **Coum-DSBDP 11** and BODIPY-distyrylBODIPY **BDP-DSBDP 7** dyads fulfill these requirements, with short separation

distances between the different chromophores and spectral overlap (Figures S25-S27). Moreover, looking at Figure 3 and the representation of the most stable conformers, the (D) and (A) transient dipole moments are not likely to be perpendicular. From these features, we can expect that the dyads should exhibit efficient Förster-resonance energy transfer. The Förster R_0 distances of the derivatives were found to be significantly greater than the donor-acceptor distances. Hence, the energy transfer efficiencies were very high, all over 99% (**Table 2**).

Table 2. Calculation Data of Energy Transfer and Förster distance

	Compound (in CH_2Cl_2)		
Parameter	**Coum-BDP 13**	**Coum-DSBDP 11**	**BDP-DSBDP 7**
J (cm^6 $mmol^{-1}$)[a]	4.4 x 10^{-14}	2.0 x 10^{-14}	1.4 x 10^{-13}
R_0 (Å)[b]	41.7	36.6	51.5
R (Å)[c]	13.7	9.1	18.2
ETE %[d]	99.9	100	99.8

[a] The overlap integral of the donor fluorescence band and the acceptor absorption band was estimated using PhotoChemCAD [69]. [b] The Förster distance was calculated using PhotoChemCAD (see supporting information), a random orientation factor was chosen κ^2 = 2/3, *n* (CH_2Cl_2) = 1.424. [c] Donor-acceptor distances were estimated from the optimized structures (Gaussian Software). [d] Energy transfer efficiency was calculated according to the following equation $\mathrm{E} = \frac{R_0^6}{R_0^6 + R^6}$.

The emission spectra of the three dyads (D-A) were compared with the emission spectra of the parent chromophores (D) under the same conditions (emission spectra were corrected for absorption at the excitation wavelength). Photoexcitation of the coumarin (D) was performed in the **Coum-BDP 13** and the **Coum-DSBDP 11** dyads at λ_{exc}=400 nm (major absorption of the coumarin and minor absorption of the DSBDP at this wavelength, figure 7) while the photoexcitation of the BODIPY (D) in the **BDP-DSBDP** dyad **7** was carried out at λ_{exc}=495 nm (exclusive absorption of BODIPY at this wavelength). A strong fluorescence

emission at 537 nm in the spectrum of the coumarin-BODIPY dyad **13** was observed, and attributed to the BODIPY moiety, while the emission of coumarin almost disappeared (Figure 8a). Similar results were obtained for the **Coum-DSBDP** dyad **11**, photoexcitation of the coumarin led to a strong fluorescence at 652 nm attributed to the distyrylBODIPY while the emission of the coumarin almost vanished (Figure 9a). Finally, in the emission spectrum of the **BDP-DSBDP** dyad **7**, a strong fluorescence emission of the distyrylBODIPY at 652 nm was observed while the emission of the BODIPY was negligible (Figure 10a). All these findings indicate the occurrence of singlet-singlet energy transfer processes from the energy donor to the energy acceptor in the coumarin (D) – BODIPY (A), the coumarin (D) - distyryl BODIPY (A) and BODIPY (D) – distyrylBODIPY (A) dyads. In the case of the coumarin (D) - distyryl BODIPY (A) the emission originates from both energy transfer and direct excitation of the acceptor. To confirm these results, the fluorescence excitation spectra of the three dyads were performed and compared to their absorption spectra (Figures 8b, 9b and 10b). The fluorescence excitation spectra of each dyad displayed the major absorption bands of the two parent chromophores. Since the emission wavelength was fixed to be selective for the acceptor, the contribution of the donor band demonstrates that EET occurs from the D to the A moiety. Moreover, for all the dyads the overlay of the excitation spectrum and absorption spectrum showed a close match throughout the spectrum that indicated a very efficient energy transfer process. This finding was confirmed by the determination of the energy transfer quantum yields (Φ_{ENT}). These Φ_{ENT} were estimated according to the equation (Φ_{ENT} = 1 - (Φ_D/ (Φ^0_D)) where Φ_D and Φ^0_D are the fluorescence quantum yields of the donor in the dyad and the donor without the acceptor, respectively. The energy transfer quantum yields were very high for **Coum-BDP 13** (Φ_{ENT} =0.978), for **Coum-DSBDP 11** (Φ_{ENT} = 0.984) and for **BDP-DSBDP 7** (Φ_{ENT} =0.987).

Table 3. Energy transfer efficiency in the dyads from steady-state measurements.

Compound	**ETE**[a]

Coum-BDP **13**	0.978
Coum-DSBDP **11**	0.984
BDP-DSBDP **7**	0.987

[a] Energy transfer efficiency determined from steady-state measurements according to the equation ($\Phi_{ENT} = 1 - (\Phi_D / (\Phi^0_D))$).

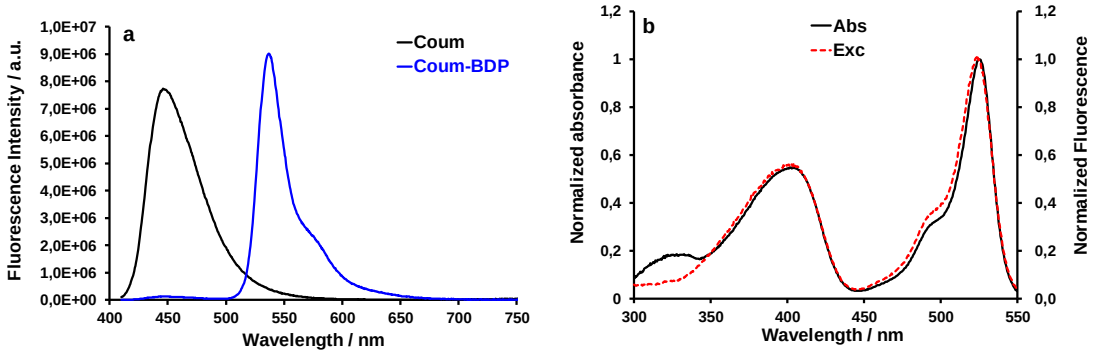

Figure 8. a) Fluorescence emission spectra of **Coum-BDP** dyad **13** (blue line) and parent chromophore coumarin **10** (black line) in dichloromethane, λ_{exc} = 400 nm, (slits 0.9 nm/0.9 nm). The emission spectra were corrected for absorption at 400 nm. b) Comparison of the UV-vis absorption and fluorescence excitation spectra of **Coum-BDP** dyad **13**, λ_{em} = 560 nm, c = 2.6 x 10^{-6} M in dichloromethane.

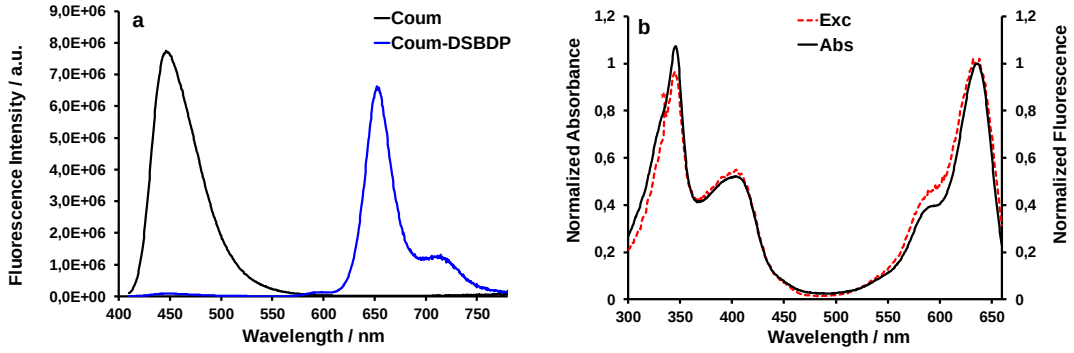

Figure 9. a) Fluorescence emission spectra of **Coum-DSBDP** dyad **11** (blue line) and parent chromophore coumarin **10** (black line) in dichloromethane, λ_{exc} = 400 nm, (slits 0.9 nm/0.9 nm). The

emission spectra were corrected for absorption at 400 nm. b) Comparison of the UV-vis absorption and fluorescence excitation spectra of **Coum-DSBDP** dyad **11**, λ_{em} = 670 nm, c = 3.0 x 10^{-6} M in dichloromethane. The peak labelled with an asterisk is due to the λexc/2.

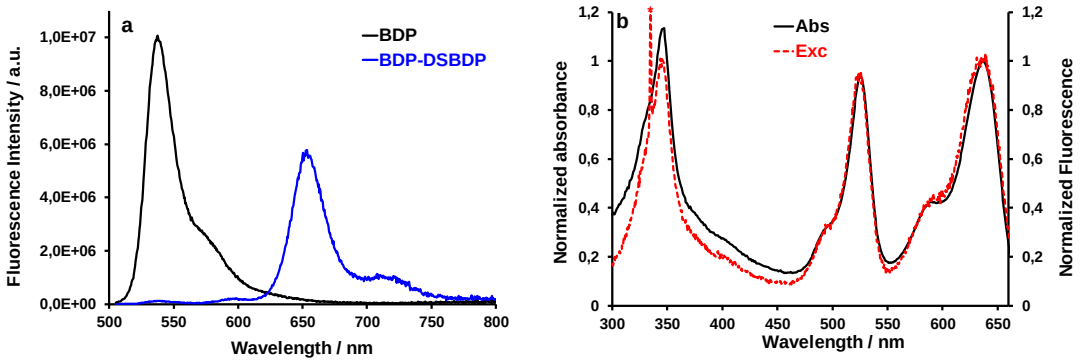

Figure 10. a) Fluorescence emission spectra of **BDP-DSBDP** dyad **7** (blue line) and parent chromophore BODIPY **BDP-alkyne** (black line) in dichloromethane, λ_{exc} = 495 nm, slits (0.9 nm/0.9 nm). The emission spectra were corrected for absorption at 495 nm. b) Comparison of the UV-vis absorption and fluorescence excitation spectra of **BDP-DSBDP** dyad **7**, λ_{em} = 670 nm, c = 1,06 x 10^{-6} M in dichloromethane. The peak labelled with an asterisk is due to the λexc/2.

Finally, we studied the fluorescence properties of the triad **Coum-BDP-DSBDP 14** in dichloromethane (Figure 11). Upon photo-excitation of the triad at λ_{exc}=400 nm (major absorption of coumarin at this wavelength with a minor contribution from DSBDP) or λ_{exc}=495 nm (exclusive absorption of BODIPY at this wavelength), fluorescence emission of the distyrylBODIPY at 653-654 nm was observed while the emission peaks from the coumarin and BODIPY almost disappeared. The fluorescence excitation spectrum of the triad was also monitored at 670 nm (DSBDP selective emission), and compared to its absorption spectrum in order to confirm the occurrence of the energy transfer process. All absorption bands of the parent chromophores were observed in the fluorescence excitation spectrum. This shows that both Coum and BDP contribute to the emission at 670nm, although they do not have

emission in this range, and are acting as energy donors. In addition, the overlay of the excitation spectrum and absorption spectrum for the triad showed a close match throughout the spectrum, which confirmed the efficiency of the energy transfer. The FRET efficiencies (Φ_{ENT} = 0.99) were determined to be more than 99% in the triad, respectively 99,3% for the coumarin and 99% for the BODIPY moiety.

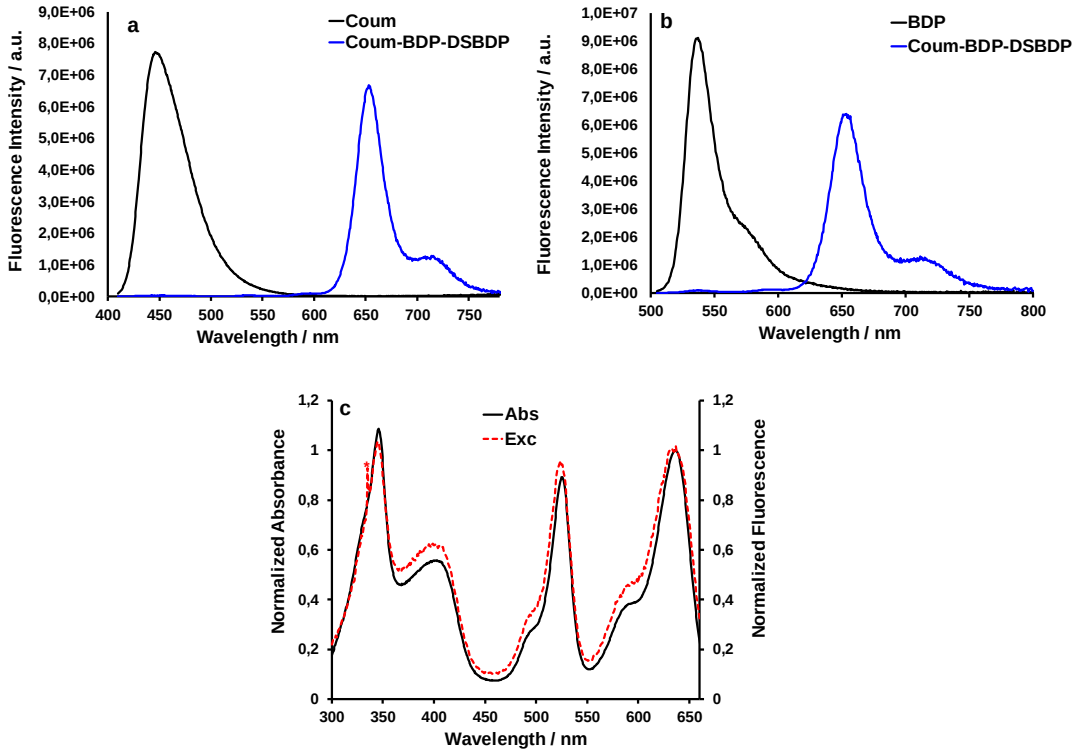

Figure 11. a) Fluorescence emission spectra of **Coum-BDP-DSBDP** triad **14** (blue line) and parent chromophore coumarin **10** (black line) in dichloromethane, λ_{exc} = 400 nm, (slits 0.9 nm/0.9 nm). The emission spectra were corrected for absorption at 400 nm. b) Fluorescence emission spectra of **Coum-BDP-DSBDP** triad **14** (blue line) and parent chromophore BODIPY **BDP-alkyne** (black line) in dichloromethane, λ_{exc} = 495 nm, (slits 0.9 nm/0.9 nm). The emission spectra were corrected for absorption at 495 nm. c) Comparison of the UV-vis absorption and fluorescence excitation spectra of **Coum-BDP-DSBDP** triad **14**, λ_{em} = 670 nm, c = 2.2 x 10^{-6} M in dichloromethane. The peak labelled with an asterisk is due to the λexc/2.

3. Conclusion

In summary, a modified α-hydroxy-β-azidotetrazole (AHBAT) scaffold bearing a piperidine moiety as an additional orthogonal attachment point was simply prepared. This trifunctional platform was used to construct three dimensional poly-chromophoric systems, by the use of sequential CuAAC reactions. A triad containing three chromophores, coumarin, BODIPY and distyrylBODIPY (**Coum-BDP-DSBDP**), and three dyads, BODIPY-distyrylBODIPY **BDP-DSBDP**, coumarin-distyrylBODIPY **Coum-DSBDP** and coumarin-BODIPY **Coum-BODIPY** were synthesized using this strategy. Computational modelling studies showed that the three chromophores were brought into close proximity within these structures. Absorption spectra and photophysical experiments were conducted on the dyads to decipher the energy transfer between each pair of chromophores, then on the **Coum-BDP-DSBDP** triad to elucidate the overall EET process in this system. The dyads and triad all exhibited FRET behaviour, with high energy transfer efficiencies. The mild conditions used to synthesize these structures are compatible with many varied chemical groups, so other donor-acceptor pairs could be combined within this scaffold. We envisage the use of dendrimeric systems incorporated onto this platform, which would allow further diversification and multiplication of the chromophores, for use as light-harvesting devices. It would also be possible to use the third substitution point to attach a selectively reactive “anchor” group for subsequent grafting to a solid support.

4. Experimental Section

4.1 General Methods

^{1}H NMR and ^{13}C NMR spectra were recorded on a Bruker Avance spectrometer (operating at 300 MHz for ^{1}H NMR and 75 MHz for ^{13}C NMR). All spectra were recorded at 25 °C, and coupling constants (*J* values) are given in hertz (Hz). Chemical shifts were given in parts per million (ppm). Splitting patterns are designated as s (singlet), d (doublet), t (triplet), q (quartet), and m (multiplet). Mass spectra were recorded on a Waters Micromass Q-TofMicro instrument. Optical measurements were performed in 10 mm path length quartz cuvettes. Absorption spectra were recorded using a Shimadzu UV-visible spectrophotometer UV-2600 in transmission mode. The emission spectra were recorded on diluted solutions (to avoid reabsorption artefacts), using a Fluoromax-4 spectrofluorimeter (Jobin-Yvon; Horiba). Corrected signals from lamp fluctuations and apparatus response functions were measured. Reactions were monitored by thin layer chromatography using Merck TLC silica gel 60F_{254} plates.

4.2 Computational details.

Gaussian 16 was used for the scans (opt=modredundant) and to optimize all the geometries at the PM3 semi-empirical level. Stationary points were verified by a harmonic vibrational frequencies calculation. A single point energy calculation at the B3LYP/6-31(+)g(d,p) level was then done to generate plots of the molecular orbitals which were visualized with GaussView 6.0 software.

4.3 Synthesis

Synthesis of distyrylBODIPY azide ***DSBDP-N$_3$.*** The BODIPY azide **BDP-N$_3$** (150 mg, 0.32 mmol) [70] was dissolved in acetonitrile (15 mL). Pyrrolidine (160 μL, 1.91 mmol) and glacial acetic acid (110 μL, 1.92 mmol) were added, then benzaldehyde (165 μL, 1.62 mmol). The mixture was heated at 80 °C for 6 h. Evaporation gave a residue that was purified by

chromatography using CH_2Cl_2/petroleum ether (2:1) as eluent. The product was isolated as a dark blue solid (100 mg, yield 49%). R_f: 0.71 (CH_2Cl_2/EP: 2/1)**.** Mp: 165-167 °C**.** ^{1}H NMR ($CDCl_3$, 300 MHz): δ 7.80 (d, 2H, *J* = 16.8 Hz, CH=CH), 7.63 (d, 4H, *J* = 7.3 Hz, ArH), 7.21-7.44 (m, 10H, ArH, CH=CH), 7.05 (d, 2H, *J* = 8.7 Hz, ArH), 4.24 (t, 2H, *J* = 4.7 Hz, CH_2O), 3.68 (t, 2H, *J* = 4.8 Hz, CH_2N_3), 2.62 (q, 4H, *J* = 7.5 Hz, CH_3CH_2), 1.40 (s, 6H, CH_3), 1.18 (t, 6H, *J* = 7.5 Hz, CH_3CH_2).^{13}C NMR ($CDCl_3$, 75 MHz): δ 158.8, 150.3, 139.1, 138.7, 137.4, 135.8, 133.9, 133.4, 129.9, 128.7, 128.6, 127.4, 120.1, 115.1, 67.0, 50.2, 18.3, 14.1, 11.7. ^{19}F NMR ($CDCl_3$, 282 MHz): δ -138.9 (q, 2F, J_{F-B} = 33Hz).^{11}B NMR ($CDCl_3$, 96 MHz): δ 2.22 (t, B, J_{F-B} = 33Hz). HRMS (ESI/Q-TOF) m/z: $[M]^+$ calcd. for $C_{39}H_{38}BF_2N_5O$ 641.3137; found 641.3152.

*Synthesis of N-Boc piperidine-4-cyanoepoxide **1**.* Sodium hydroxide (1.81 g, 45.3 mmol) was ground in a mortar and then suspended in THF (20 mL). A solution containing *N*-Boc-4-piperidone (3 g, 15.1 mmol) and chloroacetonitrile (1.15 mL, 18.1 mmol) in THF (20 mL) was added dropwise to the suspension. The mixture was stirred at room temperature for 4 h. The mixture was washed with water, then brine, dried over $MgSO_4$ and concentrated under reduced pressure. The residue was purified by chromatography using petroleum ether/ethyl acetate (75:25) as eluent. The product was isolated as a white solid (2.73 g, yield 76 %). R_f = 0.51 (EP/EtOAc: 75/25)**.** Mp: 110-112 °C. ^{1}H NMR ($CDCl_3$, 300 MHz): δ 3.71-3.82 (m, 2H, CH_2N); 3.44-3.53 (m, 2H, CH_2N); 3.35 (s, 1H, OC*H*CN); 1.97-2.04 (m, 1H, CH*H*); 1.66-1.82 (m, 2H, CH_2); 1.48 (m, 10H, CH_3C, CH*H*). ^{13}C NMR ($CDCl_3$, 75 MHz): δ 154.4, 115.5, 80.3, 63.6, 47.0, 42.1, 32.5, 30.6, 28.3. HRMS (ESI/Q-TOF) m/z: [M - Boc + H] $^+$ calcd. for $C_7H_{11}N_2O$ 139.0871; found 139.0867.

*Synthesis of N-Boc piperidine α-hydroxy-β-azidotetrazole **2**.* A solution of cyanoepoxide **1** (0.60 g, 2.5 mmol), Bu_2SnO (0.31 g, 1.25 mmol) and $TMSN_3$ (1.3 mL, 7.5 mmol) in toluene (25 mL, 7.5 mmol) was stirred at 60 °C for 18 h. The solvent was removed under reduced pressure. A THF (35 mL)/2N aqueous HCl (1.5 mL) mixture was added to the residue and stirred for 30 minutes. Water and EtOAc were added, and the phases separated. The

aqueous layer was extracted twice with EtOAc. The combined organic phases were washed with brine, dried over $MgSO_4$ and concentrated under reduced pressure. The residue was purified by chromatography using dichloromethane/ MeOH /acetic acid (94.5:5:0.5) as eluent. The product was isolated as a white solid (511 mg, yield 63 %). R_f = 0.48 (EtOAc/AcOH: 99/1)**.** Mp: 168-170 °C. ^{1}H NMR (DMSO-d_6, 300 MHz): δ 6.88 (d, 1H, *J* = 4.6 Hz, C*H*OH), 5.10 (d, 1H, *J* = 4.5 Hz, CHO*H*), 3.76-3.93 (m, 2H, CH_2N), 2.84 (bs, 2H, CH_2N), 1.96-2.00 (bd, 1H, *J* = 13.7 Hz, CH*H*), 1.68-1.78 (m, 1H, CH*H*), 1.38- 1.52 (m, 1H, CH*H*), 1.38 (s, 9H, C*H*$_3$C), 1.17-1.22 (bd, 1H, *J* = 14.6 Hz, CH*H*). ^{13}C NMR (DMSO-d_6, 75 MHz): δ 156.0, 153.8, 78.9, 71.2, 64.1, 30.0, 29.5, 28.1. HRMS (ESI/Q-TOF) m/z: $[M + Na]^+$ calcd for $C_{12}H_{20}N_8O_3Na$ 347.1556**;** found 347.1562**.**

*Synthesis of N-Fmoc piperidine α-hydroxy-β-azidotetrazole **3**.* A solution of compound **2** (199 mg, 0.61 mmol) in CH_2Cl_2 (7 mL) was cooled to 0 °C then trifluoroacetic acid (1 mL) was added. The mixture was stirred at 0 °C for 1.5 h and concentrated. To this residue, THF (7 mL) and H_2O (7 mL) were added. The mixture was cooled to 0 °C then $NaHCO_3$ (113 mg, 1.34 mmol) and Fmoc-*N*-hydroxysuccinimide (257 mg, 0.763 mmol) were added. The mixture was stirred at 0 °C for 1.5 h then at room temperature over night. Evaporation gave a residue that was purified by flash chromatography over silica gel using CH_2Cl_2/MeOH/AcOH (96.5:3:0.5) as eluent to give the product as a white solid (234 mg, yield 86 %). R_f = 0.55 (EtOAc/1 % AcOH). Mp: 140-142 °C**.** ^{1}H NMR (DMSO-d_6, 300 MHz): δ 7.89 (d, 2H, *J* = 7.4 Hz, ArH), 7.62 (d, 2H, *J* = 7.3 Hz, ArH), 7.31-7.44 (m, 4H, ArH), 6.81 (bs, 1H, C*H*OH), 5.05 (s, 1H, CHO*H*), 4.38 (b, 2H, CH_2O), 4.27 (t, 1H, *J* = 6.1 Hz, C*H*CH_2O), 3.62-3.99 (m, 2H, CH_2N), 2.75-2.94 (m, 2H CH_2N), 1.86-1.95 (m, 1H, CH*H*), 1.53-1.66 (m, 1H, CH*H*), 1.36-1.46 (m, 1H, CH*H*), 1.15-30 (m, 1H, CH*H*). ^{13}C NMR (DMSO-d_6, 75 MHz): δ 156.2, 154.2, 143.8, 140.8, 127.6, 127.1, 125.0, 120.1, 71.3, 66.5, 64.1, 46.8, 29.8, 29.5. HRMS (ESI/Q-TOF) m/z: $[M + H]^+$ calcd for $C_{22}H_{23}N_8O_3$ 447.1893; found 447.1886.

*Synthesis of triazole **4**.* Compound **3** (90 mg, 0.2 mmol), BODIPY-alkyne (95 mg, 0.22 mmol) and TBTA (12 mg, 0.022 mmol) were dissolved in THF (3 mL). $CuSO_4 \cdot 5H_2O$ (5 mg, 0.02

mmol) and sodium ascorbate (12 mg, 0.06 mmol), each dissolved in H_2O (0.5 mL), were added to the mixture. The mixture was stirred at room temperature for 3 days. Evaporation gave a residue that was purified by flash chromatography using ethyl acetate/1% AcOH as eluent. The product was isolated as an orange solid (133 mg, Yield 76 %). R_f = 0.29 (EtOAc/AcOH: 99/1)**.** Mp: 228-230 °C**.** ^{1}H NMR ($CDCl_3$, 300 MHz): δ 7.73 (d, 2H, *J* = 9Hz, ArH), 7.52 (d, 2H, *J* = 9Hz, ArH), 7.30-7.43 (m, 4H, ArH, CH), 7.17- 7.20 (m, 5H, ArH), 7.15 (d, 2H, *J* = 9.0 Hz, ArH), 7.02 (d, 2H, *J* = 9.0 Hz, ArH), 5.35 (s, 1H, C*H*OH), 5.13 (s, 2H, CH_2O), 4.46 (bs, 2H, CHC*H*$_2$O), 4.19 (t, 1H, *J* = 5.9 Hz, C*H*CH_2O), 2.63-2.85 (m, 4H, CH_2N), 2.52 (s, 6H, CH_3), 2.26 (q, 4H, *J* = 6.0 Hz, C*H*$_2CH_3$), 2.13-2.17 (m, 4H, CH_2), 1.26 (s, 6H, CH_3), 0.95 (t, 6H, *J* = 6.0 Hz, C*H*$_3CH_2$).^{13}C NMR ($CDCl_3$, 75 MHz): δ 158.3, 155.3, 153.7, 143.6, 141.3, 139.6, 138.1, 137.8, 132.8, 131.0, 129.8, 129.0, 128.2, 127.1, 125.3, 124.8, 120.1, 115.1, 67.6, 66.2, 61.6, 47.3, 39.5, 17.0, 14.6, 12.5, 11.8. HRMS (ESI/Q-TOF) m/z: [M + Na]$^+$ calcd for $C_{48}H_{51}BF_2N_{10}O_4Na$, 903.4054; found 903.4083.

*Synthesis of alkyne **5***. Compound **4** (102 mg, 0.12 mmol) was dissolved in dichloromethane (6 mL) and EDC (19 mg, 0.099 mmol) was added. The mixture was stirred at room temperature for 18 h. The mixture was washed with a solution of saturated aqueous NaCl and dried by filtering through phase separator filter paper. The filtrate was evaporated and purified by flash chromatography using CH_2Cl_2/AcOEt (9:1) as eluent. The product was isolated as an orange solid (58 mg, yield 62 %). R_f = 0.65 (CH_2Cl_2/AcOEt: 9/1). Mp: 158-160 °C**.** ^{1}H NMR ($CDCl_3$, 300 MHz): 8.07 (s, 1H, CH), 7.77 (d, 2H, *J* = 9.0 Hz, ArH), 7.60 (d, 2H, *J* = 9.0 Hz, ArH), 7.31-7.44 (m, 4H, ArH), 7.20 (d, 2H, *J* = 8.0 Hz, ArH), 7.13 (d, 2H, *J* = 8.0 Hz, ArH), 5.29 (s, 2H, CH_2O), 4.49-4.60 (m, 2H, CHC*H*$_2$O), 4.23-4.36 (m, 2H, C*H*CH_2O, CH*H*N), 4.01-4.17 (m, 1H, CH*H*N), 3.25-3.33 (m, 2H, CH_2N), 2.86 (s, 1H, CH≡), 2.54 (s, 6H, CH_3), 2.38-2.49 (m, 2H, CH_2), 2.31 (q, 4H, *J* = 7.7 Hz, C*H*$_2CH_3$), 2.12-2.25 (m, 2H, CH_2), 1.34 (s, 6H, CH_3), 0.99 (t, 6H, *J* = 7.4 Hz, C*H*$_3CH_2$). ^{13}C NMR ($CDCl_3$, 75 MHz): δ 158.7, 154.8, 153.6, 143.8, 143.1, 141.4, 139.9, 138.3, 132.7, 131.1, 129.6, 128.6, 127.7, 127.1, 124.8,

121.7, 120.0, 115.2, 80.4, 77.6, 67.3, 62.0, 59.7, 47.4, 40.9, 37.6, 17.1, 14.6, 12.5, 11.8. HRMS (ESI/Q-TOF) m/z: $[M]^+$ calcd for $C_{48}H_{49}BF_2N_6O_3$, 806.3927; found 806.3946.

*Synthesis of bis-triazole **6**.* Compound **5** (50 mg, 0.06 mmol), **DSBDP-N_3** (44 mg, 0.07 mmol) and TBTA (4 mg, 0.007 mmol) were dissolved in THF (2 mL). $CuSO_4 \cdot 5H_2O$ (2 mg, 0.006 mmol) and sodium ascorbate (5 mg, 0.02 mmol), each dissolved in H_2O (0.25 mL), were added to the mixture. The mixture was stirred for 18 h. Evaporation gave a residue that was purified by flash chromatography using CH_2Cl_2/EtOAc (95:5) then CH_2Cl_2/EtOAc (90:10) and CH_2Cl_2/EtOAc (87.5:12.5) as eluent. The product was isolated as a dark blue solid (77 mg, yield 86 %). R_f: 0.1 (EP/ EtOAc: 75/25)**.** Mp: 205-207 °C. ^{1}H NMR ($CDCl_3$, 300 MHz): δ 7.75-7.90 (m, 5H, ArH, CH), 7.57-7.69 (m, 7H, ArH), 7.18-7.43 (m, 16H, ArH), 7.11 (d, 2H, *J* = 8.6 Hz, ArH), 6.98 (d, 2H, *J* = 8.5 Hz, ArH), 5.24 (s, 2H, CH_2O), 4.72-4.75 (m, 2H,NCH_2CH_2O), 4.49-4.57 (m, 2H, $CHCH_2O$), 4.37-4.45 (m, 2H, NCH_2CH_2O), 4.24 (t, 1H, *J* = 6.1 Hz, $CHCH_2O$), 3.51-3.60 (m, 4H, CH_2N), 2.48-2.86 (m, 14H, CH_3, CH_2, CH_2CH_3), 2.30 (q, 4H, *J* = 7.4 Hz, CH_2CH_3), 1.35 (s, 6H, CH_3), 1.33 (s, 6H, CH_3), 1.17 (t, 6H *J* = 7.3 Hz, CH_3CH_2), 0.99 (t, 6H, *J* = 7.4 Hz, CH_3CH_2). ^{13}C NMR ($CDCl_3$, 75 MHz): δ 158.6, 158.2, 154.9, 153.5, 150.3, 149.0, 143.7, 141.3, 139.8, 138.9, 138.2, 137.1, 135.9, 133.8, 133.2, 132.6, 131.0, 130.0, 129.5, 129.1, 128.7, 128.6, 127.6, 127.3, 127.0, 124.7, 122.7, 121.4, 119.9, 115.1, 67.0, 66.1, 61.9, 60.3, 49.9, 47.3, 40.1, 34.7, 18.2, 17.0, 14.5, 14.0, 12.4, 11.7. HRMS (ESI/Q-TOF) m/z: $[M]^+$ calcd for $C_{87}H_{87}B_2F_4N_{11}O_4Na$ 1447.7065; found 1447.7089.

*Synthesis of BODIPY–distyrylBODIPY dyad **7**.* Compound **6** (29 mg, 0.02 mmol) was dissolved in dichloromethane (4 mL) and diethylamine (0.5 mL) was added. The mixture was stirred at rt for 24 h. Evaporation gave a residue that was purified by flash chromatography using CH_2Cl_2/MeOH (92.5:7.5) as eluent. The product was isolated as a dark blue solid (21 mg, yield 85 %). R_f: 0.3 (CH_2Cl_2/MeOH: 90/10). Mp: 173-176°C. ^{1}H NMR ($CDCl_3$, 300 MHz): 7.93 (s, 1H, CH), 7.72-7.82 (m, 3H, ArH, CH, CH=), 7.62-7.64 (m, 4H, ArH), 7.38-7.43 (m, 4H, ArH, CH=), 7.26-7.34 (m, 3H, ArH), 7.18-7.23 (m, 5H, ArH), 7.08 (d, 2H, *J* = 8.9 Hz, ArH), 6.98 (d, 2H, , *J* = 8.8 Hz, ArH), 5.22 (s, 2H, CH_2O), 4.76 (t, 2H, *J* = 4.7 Hz,

NCH_2CH_2O), 4.43 (t, 2H, *J* = 4.5 Hz, NCH_2CH_2O), 3.88 (bs, 1H, NH), 3.06-3.15 (m, 3H, CH_2N, C*H*H), 2.87-2.96 (m, 3H, CH_2N, C*H*H), 2.62 (q, 4H, *J* = 7.4 Hz, CH_2CH_3), 2.53 (s, 6H, CH_3), 2.30 (q, 4H, *J* = 7.3 Hz, CH_2CH_3), 1.24-1.38 (m, 14H, CH*H*, CH_3), 1.16 (t, 6H, *J* = 7.3 Hz, CH_3CH_2), 0.98 (t, 6H, *J* = 7.4 Hz, CH_3CH_2). δ ^{13}C NMR ($CDCl_3$, 75 MHz): δ 158.6, 158.2, 153.5, 150.4, 149.4, 143.7, 138.9, 138.3, 137.2, 135.9, 133.8, 133.3, 132.7, 131.0, 130.0, 129.6, 129.2, 128.7, 128.6, 128.5, 127.3, 122.7, 121.4, 120.0, 115.1, 66.1, 62.0, 60.1, 49.9, 41.7, 35.0, 29.6, 18.3, 17.0, 14.6, 14.0, 12.4, 11.8. HRMS (ESI/Q-TOF) m/z: $[M + H]^+$ calcd for $C_{72}H_{78}B_2F_4N_{11}O_2$, 1226.6462; found 1226.6495.

Synthesis of N-(7-diethylamino)coumarin piperidine α-hydroxy-β-azidotetrazole ***8****.* A solution of compound **2** (162 mg, 0.5 mmol) in CH_2Cl_2 (5 mL) was cooled to 0°C then trifluoroacetic acid (0.7 mL) was added. The mixture was stirred at 0 °C for 90 min and then concentrated under reduced pressure. 7-(Diethylamino)coumarin-3-carboxylic acid (130 mg, 0.5 mmol) was suspended in THF (3 mL) and cooled to 0 °C. Ethyl chloroformate (0.05 mL, 0.5 mmol) and triethylamine (0.07 mL, 0.5 mmol) were added, and the mixture was stirred at 0 °C for 2 h. The deprotected amine residue was dissolved in EtOH (2 mL) and added to this mixture, along with triethylamine (0.15 mL, 1.1 mmol). The mixture was stirred at 0°C over night. Evaporation gave a residue that was purified by flash chromatography using CH_2Cl_2 /MeOH/AcOH 95:5:2 as eluent. The product was isolated as a yellow solid (139 mg, yield 59 %). R_f: 0.24 (CH_2Cl_2/MeOH/AcOH 90:10:1)**.** Mp: 146-148 °C**.** ^{1}H NMR (CD_3OD, 300 MHz): δ 7.90 (s, 1H, ArH), 7.42 (d, 1H, *J* = 8.9 Hz, ArH), 6.74 (dd, 1H, *J* = 2.0 Hz, 8.9 Hz, ArH), 6.54 (bs, 1H, ArH), 5.11 (s, 1H, C*H*OH), 4.43-4.61 (m, 1H, C*H*HN), 3.58-3.76 (m, 1H, CH*H*N), 3.50 (q, 4H, *J* = 7.0 Hz, NCH_2CH_3), 3.35 (m, 1H C*H*HN), 2.96-3.09 (m, 1H CH*H*N), 2.13-2.31 (m, 1H, C*H*H), 1.72-1.79 (m, 1H, C*H*H), 1.22-1.42 (b, 2H, CH*H*), 1.21 (t, 6H, *J* = 6.9 Hz, NCH_2CH_3). ^{13}C NMR (CD_3OD, 75 MHz): δ. 167.3, 161.4, 158.7, 158.0, 153.7, 146.2, 131.5, 116.5, 111.2, 109.1, 97.8, 73.6, 65.5, 45.9, 45.0, 44.7, 39.5, 32.5, 31.7, 31.1, 12.8. HRMS (ESI/Q-TOF) m/z: $[M + H]^+$ calcd for $C_{21}H_{26}N_9O_4$ 468.2108; found 468.2104.

*Synthesis of triazole **9**.* Compound **8** (135 mg, 0.29 mmol), 1-octyne (60 µL, 0.43 mmol) and TBTA (17.5 mg, 0.033 mmol) were dissolved in THF (3 mL) and nBuOH (1 mL). $CuSO_4 \cdot 5H_2O$ (7.5 mg, 0.03 mmol) and sodium ascorbate (18 mg, 0.09 mmol), each dissolved in H_2O (0.8 mL), were added. The mixture was stirred at room temperature for 3 days. Evaporation gave a residue that was purified by chromatography using EtOAc/AcOH 98:2 as eluent. The product was isolated as a yellow solid (137 mg, yield 82 %). R_f: 0.28 (EtOAc/AcOH 99:1)**.** Mp: 155-157 °C**.** ^{1}H NMR (CD_3OD, 300 MHz): δ 7.89 (s, 1H, ArH), 7.78 (d, 1H, *J* = 9.1 Hz, CH), 7.43 (d, 1H, *J* = 8.9 Hz, ArH), 6.74-6.78 (dd, 1H, *J* = 2.4 Hz, 8.9 Hz, ArH), 6.56 (d, 1H, *J* = 2.2 Hz, ArH), 5.22 (s, 1H, C*H*OH), 4.58 (bd, 1H, *J* = 12.7 Hz, C*H*HN), 3.72 (bd, 1H, *J* = 12.2 Hz, C*H*HN), 3.51 (q, 4H, *J* = 7.0 Hz, NC*H*$_2$CH$_3$), 2.78-3.06 (m, 4H, CH*H*N, C*H*H), 2.67 (t, 2H, *J* = 7.5 Hz, CH_2), 2.23-2.40 (m, 2H, CH*H*), 1.61-1.68 (m, 2H, CH_2), 1.33 (b, 6H, CH_2), 1.22 (t, 6H, *J* = 7.0 Hz, NCH$_2$C*H*$_3$), 0.90 (t, 3H, *J* = 6.5 Hz, CH_3). ^{13}C NMR (CD_3OD, 75 MHz): δ 167.3, 161.4, 158.7, 153.7, 149.3, 146.2, 131.5, 123.2, 116.5, 111.2, 109.1, 97.9, 73.0, 67.4, 46.0, 44.6, 39.1, 32.9, 32.1, 30.5, 30.1, 26.6, 23.7, 14.6, 12.8. HRMS (ESI/Q-TOF) m/z: $[M + H]^+$ calcd for $C_{29}H_{40}N_9O_4$ 578.3203; found 578.3207.

*Synthesis of alkyne **10**.* Compound **9** (120 mg, 0.21 mmol) was dissolved in CH_2Cl_2 (10 mL) and EDC (54 mg, 0.28 mmol) was added. The mixture was stirred at rt for 24 h. Evaporation gave a residue that was purified by chromatography using CH_2Cl_2 /MeOH 97:3 as eluent. The product was isolated as a yellow solid (42 mg, yield 42 %). R_f: 0.33 (CH_2Cl_2 /MeOH 97:3)**.** Mp: 71-73 °C**.** ^{1}H NMR ($CDCl_3$, 300 MHz): δ 7.90 (s, 1H, ArH), 7.65 (s, 1H, CH), 7.32 (d, 1H, 8.9 Hz, ArH), 6.61-6.65 (dd, 1H, *J* = 2.4 Hz, 8.9 Hz, ArH), 6.50 (d, 1H, *J* = 2.2 Hz, ArH), 4.73 (bd, 1H, *J* = 12.0 Hz, C*H*HN), 3.64-3.78 (m, 2H, C*H*HN, CH*H*N), 3.45 (q, 4H, *J* = 7.0 Hz, NC*H*$_2$CH$_3$), 3.32-3.42 (m, 1H, CH*H*N), 2.83 (s, 1H, CH≡), 2.72 (t, 2H, *J* = 7.5 Hz, CH_2), 2.50-2.58 (m, 2H, C*H*H), 2.23-2.33 (m, 2H, CH*H*), 1.62-1.72 (m, 2H, CH_2), 1.30-1.39 (m, 6H, CH_2), 1.22 (t, 6H, *J* = 7.0 Hz, NCH$_2$C*H*$_3$), 0.88 (t, 3H, *J* = 6.7 Hz, CH_3). ^{13}C NMR ($CDCl_3$, 75 MHz): δ 164.9, 159.1, 157.2, 151.6, 145.2, 129.9, 119.2, 116.1, 109.6, 108.0,

97.2, 80.8, 59.2, 45.1, 44.4, 39.0, 38.0, 31.5, 29.3, 28.9, 25.6, 22.5, 14.0, 12.3. HRMS (ESI/Q-TOF) m/z: $[M + H]^+$ calcd for $C_{29}H_{38}N_5O_3$ 504.2975; found 504.2978.

*Synthesis of coumarin–distyrylBODIPY dyad **11**.* Compound **10** (20 mg, 0.04 mmol), **DSBDP-N_3** (31 mg, 0.05 mmol) and TBTA (3 mg, 0.005 mmol) were dissolved in THF (1 mL). $CuSO_4 \cdot 5H_2O$ (1 mg, 0.004 mmol) and sodium ascorbate (2 mg, 0.012 mmol), each dissolved in H_2O (0.1 mL), were added. The mixture was stirred at room temperature for 3 days. Evaporation gave a residue that was purified by chromatography using CH_2Cl_2/MeOH 97:3 as eluent. The product was isolated as a dark blue solid (36 mg, yield 81 %). R_f: 0.29 (CH_2Cl_2/MeOH 97:3)**.** Mp: 142-144 °C**.** ^{1}H NMR ($CDCl_3$, 300 MHz): δ 7.85 (s, 1H, ArH), 7.82 (s, 1H, CH), 7.77 (s, 1H, CH), 7.62-7.67 (m, 5H, ArH, CH=), 7.53 (s, 1H, ArH), 7.20-7.43 (m, 13H, ArH, CH=), 6.98 (d, 1H, 8.6 Hz, ArH), 6.58-6.61 (dd, 1H, *J* = 2.3 Hz, 8.8 Hz, ArH), 6.48 (d, 1H, *J* = 2.2 Hz, ArH), 5.53 (s, 1H), 4.77 (t, 2H, *J* = 4.9 Hz, NCH_2CH_2O), 4.43 (t, 2H, *J* = 4.9 Hz, NCH_2CH_2O), 4.02-4.07 (b, 2H, CH_2N), 3.54-3.71 (b, 2H, CH_2N), 3.43 (q, 4H, *J* = 7.2 Hz, NCH_2CH_3), 2.79-2.98 (m, 4H, CH_2), 2.58-2.72 (m, 6H, CH_2), 1.60-1.70 (m, 2H, CH_2), 1.29-1.36 (m, 11H, CH_2, CH_3), 1.14-1.24 (m, 12H, NCH2C*H3*, CH2C*H3*), 0.87 (t, 3H, *J* = 6.7 Hz, CH_3). ^{13}C NMR ($CDCl_3$, 75 MHz): δ 165.0, 159.2, 158.2, 157.2, 151.7, 150.4, 149.8, 148.7, 145.2, 139.1, 138.4, 137.3, 135.8, 133.9, 133.3, 130.0, 129.2, 129.1, 128.8, 128.7, 128.6, 128.0, 127.3, 122.6, 120.1, 119.0, 116.0, 115.1, 109.4, 107.7, 96.9, 66.1, 59.9, 54.3, 49.9, 44.9, 43.8, 38.3, 35.2, 31.5, 29.3, 29.0, 25.7, 22.5, 18.3, 14.0, 12.4, 11.8. HRMS (ESI/Q-TOF) m/z: $[M]^+$ calcd for $C_{68}H_{75}BF_2N_{10}O_4$ 1144.6034; found 1144.6056.

*Synthesis of triazole **12**.* Compound **8** (95 mg, 0.2 mmol), BDP-alkyne (95 mg, 0.22 mmol) and TBTA (18 mg, 0.033 mmol) were dissolved in THF (3 mL). $CuSO_4 \cdot 5H_2O$ (7.5 mg, 0.03 mmol) and sodium ascorbate (18 mg, 0.09 mmol), each dissolved in H_2O (0.5 mL), were added. The mixture was stirred at room temperature for 2 days. Evaporation gave a residue that was purified by flash chromatography using CH_2Cl_2/MeOH/AcOH 95:5:2 as eluent. The product was isolated as an orange solid (153 mg, yield 85 %). R_f: 0.41 (CH_2Cl_2/MeOH/AcOH 95:5:1)**.** Mp: 230 °C (dec)**.** ^{1}H NMR (CD_3OD:$CDCl_3$, 300 MHz): δ 8.16 (d, 1H, *J* = 8.1 Hz,

CH), 7.84 (s, 1H, ArH), 7.39 (d, 1H, *J* = 8.9 Hz, ArH), 7.15-7.21 (m, 4H, ArH), 6.70-6.74 (dd, 1H, *J* = 2.3 Hz, 8.9 Hz, ArH), 6.52 (d, 1H, *J* = 1.5 Hz, ArH), 5.25 (s, 3H, CH_2O, C*H*OH), 4.55-4.59 (m, 1H, C*H*HN), 3.68-3.74 (m, 1H, C*H*HN), 3.49 (q, 4H, *J* = 6.8 Hz, NC*H*$_2$CH$_3$), 2.68-3.11 (m, 4H, CH*H*N, C*H*H), 2.47 (s, 6H, CH_3), 2.31 (q, 6H, *J* = 7.4 Hz, C*H2*CH3, CH*H*), 1.34 (s, 6H, CH*3*), 1.21 (t, 6H, *J* = 7.0 Hz, NCH$_2$C*H*$_3$), 0.97 (t, 6H, *J* = 7.4 Hz, CH2C*H3*). ^{13}C NMR (CD_3OD: $CDCl_3$, 75 MHz): δ 167.0, 161.1, 160.2, 158.5, 154.5, 153.5, 151.9, 141.8, 139.7, 133.9, 132.3, 131.3, 130.7, 129.4, 125.4, 116.7, 116.1, 115.0, 111.1, 108.9, 97.7, 67.6, 62.6, 45.9, 17.8, 15.1, 12.8, 12.7, 12.3. HRMS (ESI/Q-TOF) m/z: $[M]^+$ calcd for $C_{47}H_{54}BF_2N_{11}O_5$ 901.4371; found 901.4415.

*Synthesis of coumarin–BODIPY dyad **13**.* Compound **12** (123 mg, 0.14 mmol) was dissolved in CH_2Cl_2 (7 mL) and EDC (37 mg, 0.19 mmol) was added. The mixture was stirred at rt for 24 h. The mixture was diluted with CH_2Cl_2, washed with a solution of saturated aqueous NaCl and dried by filtering through phase separator filter paper. The filtrate was evaporated and purified by chromatography using CH_2Cl_2/EtOAc (8:2) as eluent. The product was isolated as an orange solid (75 mg, yield 67 %). R_f = 0.34 (CH_2Cl_2/EtOAc: 8:2). Mp: 256 °C (dec)**.** ^{1}H NMR ($CDCl_3$, 300 MHz): δ 8.08 (s, 1H, CH), 7.93 (s,1H, ArH), 7.35 (d, 1H, *J* = 8.8 Hz, ArH), 7.18 (d, 2H, *J* = 8.7 Hz, ArH), 7.13 (d, 2H, *J* = 8.7 Hz, ArH), 6.65-6.69 (dd, 1H, *J* = 2.3 Hz, 8.8 Hz, ArH), 6.53 (d, 1H, *J* = 2.3 Hz, ArH), 5.27 (s, 2H, CH_2O), 4.76-4.80 (m, 1H, C*H*HN), 3.66-3.81 (m, 2H, C*H*HN, CH*H*N), 3.46 (q, 4H, *J* = 7.2 Hz, NC*H*$_2$CH$_3$), 3.33-3.38 (m, 1H, CH*H*N), 2.88 (s, 1H, CH≡), 2.60-2.68 (m, 2H, C*H*H), 2.53 (s, 6H, CH_3), 2.32 (q, 6H, *J* = 7.4 Hz, C*H*$_2$CH$_3$, CH*H*), 1.33 (s, 6H, CH_3), 1.24 (t, 6H, *J* = 7.2 Hz, NCH$_2$C*H*$_3$), 0.98 (t, 6H, *J* = 7.4 Hz, CH$_2$C*H*$_3$). ^{13}C NMR ($CDCl_3$, 75 MHz): δ 164.9, 159.0, 158.6, 157.2, 153.5, 151.4, 145.4, 143.2, 140.0, 138.3, 132.7, 131.1, 130.0, 129.6, 128.6, 121.6, 116.3, 115.3, 109.9, 108.3, 100.2, 97.5, 80.5, 77.9, 62.0, 59.8, 45.3, 44.4, 39.0, 38.1, 17.0, 14.6, 12.4, 12.3, 11.8. HRMS (ESI/Q-TOF) m/z: $[M]^+$ calcd for $C_{47}H_{52}BF_2N_7O_4$ 827.4142; found 827.4136.

*Synthesis of coumarin–BODIPY–distyrylBODIPY triad **14**.* Compound **13** (55 mg, 0.066 mmol), **DSBDP-N$_3$** (50 mg, 0.08 mmol) and TBTA (4 mg, 0.008 mmol) were dissolved in THF

(2 mL). $CuSO_4 \cdot 5H_2O$ (1.7 mg, 0.007 mmol) and sodium ascorbate (4 mg, 0.021 mmol), each dissolved in H_2O (0.25 mL), were added. The mixture was stirred at room temperature for 24 h. Evaporation gave a residue that was purified by chromatography using CH_2Cl_2 /EtOAc 75:25 as eluent. The product was isolated as a dark blue solid (84 mg, yield 87 %). R_f: 0.40 (CH_2Cl_2/EtOAc 7:3)**.** Mp: 203-205°C**.** ^{1}H NMR ($CDCl_3$, 300 MHz): δ 7.98 (s, 1H, CH), 7.87 (s, 1H, ArH), 7.76-7.82 (m, 3H, CH, CH=), 7.62 (d, 4H, *J* = 7.4 Hz, ArH), 7.38-7.43 (m, 4H, ArH), 7.18-7.34 (m, 9H, ArH, CH=), 7.11 (d, 2H, *J* = 8.7 Hz, ArH), 7.02 (d, 2H, *J* = 8.7 Hz, ArH), 6.59-6.63 (dd, 1H, *J* = 2.3 Hz, 8.9 Hz, ArH), 6.49 (d, 1H, *J* = 2.2 Hz, ArH), 5.23 (s, 2H, CH_2O), 4.80 (t, 2H, *J* = 4.6 Hz, $NCH_2C\mathit{H}_2O$), 4.46 (t, 2H, *J* = 4.7 Hz, $NC\mathit{H}_2CH_2O$), 3.73-4.04 (m, 2H, C*H*HN), 3.57 (b, 2H, CH*H*N), 3.43 (q, 4H, *J* = 6.9 Hz, $NC\mathit{H}_2CH_3$), 2.90-3.03 (m, 4H, CH_2), 2.62 (q, 4H, *J* = 6.8 Hz, $C\mathit{H}_2CH_3$), 2.53 (s, 6H, CH_3), 2.28 (q, 4H, *J* = 7.4 Hz, $C\mathit{H}_2CH_3$), 1.37 (s, 6H, CH_3), 1.32 (s, 6H, CH_3), 1.14-1.26 (m, 12H, $CH_2C\mathit{H}_3$, $NCH_2C\mathit{H}_3$), 0.98 (t, 6H, *J* = 7.4 Hz, $CH_2C\mathit{H}_3$). ^{13}C NMR ($CDCl_3$, 75 MHz): δ 165.0, 159.3, 158.7, 158.2, 157.3, 153.5, 151.8, 150.4, 149.2, 145.4, 143.8, 139.9, 139.0, 138.4, 137.3, 135.9, 133.9, 133.3, 132.7, 131.1, 130.1, 129.9, 129.6, 129.3, 128.7, 128.6, 127.3, 122.7, 121.5, 120.0, 115.8, 115.2, 109.5, 107.8, 96.9, 66.2, 62.0, 60.5, 50.0, 45.0, 43.8, 38.4, 35.0, 18.3, 17.0, 14.6, 14.0, 12.5, 12.4, 11.8. HRMS (ESI/Q-TOF) m/z: $[M + Na]^+$ calcd for $C_{86}H_{90}B_2F_4N_{12}O_5Na$, 1491.7177; found 1491.7220.

Declaration of competing interest

The authors declare that they have no known competing financial interests or personal relationships that could have appeared to influence the work reported in this paper.

CRediT authorship contribution statement

Assia Tafrioucht: Methodology, Investigation. Jad Rabah: Methodology, Investigation. Krystyna Baczko: Investigation, Data curation. Hélène Fensterbank Methodology, Data curation. Rachel Méallet-Renault: Methodology, Investigation, Writing - review & editing. Gilles Clavier: Investigation, Conceptualization, Writing - review & editing. François Couty:

Conceptualization, Project administration. Emmanuel Allard: Investigation, Writing – review & editing, Project administration, Supervision. Karen Wright: Conceptualization, Methodology, Investigation, Writing - review & editing, Project administration, Supervision.

Acknowledgments:

This work was granted access to the HPC resources of CINES under the allocation 2019-A0050810547 made by GENCI and to the HPC resources from the “Mésocentre” computing center of CentraleSupélec and École Normale Supérieure Paris-Saclay supported by CNRS and Région Île-de-France (http://mesocentre.centralesupelec.fr/). JR thanks the « Ministère de l’Enseignement Supérieur de la Recherche et de l’Innovation » for a PhD fellowship. RMR thanks the Région Ile-de-France and DIM NanoK for financial support. The University of Versailles St-Quentin-en-Yvelines, University Paris-Saclay and the CNRS are acknowledged for funding.

Dedication

This paper is dedicated to the memory of Professor François Couty (1963-2019), whose love of organic chemistry inspired his students and colleagues.

References

[1] Beal, D. M.; Jones, L. H. Molecular scaffolds using multiple orthogonal conjugations: applications in chemical biology and drug discovery. *Angew. Chem. Int. Ed*. **2012**, *51*, 6320-6.

[2] Vaněk, V.; Pícha, J.; Fabre, B.; Buděšínský, M.; Lepšík, M.; Jiráček, J. The development of a versatile trifunctional scaffold for biological applications. *Eur. J. Org. Chem*. **2015**, 3689-701.

[3] Yoshida, S.; Kanno, K.; Kii, I.; Misawa, Y.; Hagiwara, M.; Hosoya, T. Convergent synthesis of trifunctional molecules by three sequential azido-type-selective cycloadditions. *Chem. Commun.* **2018**, *54*, 3705-8.

[4] Meguro, T.; Sakata, Y.; Morita, T.; Hosoya, T.; Yoshida, S. Facile assembly of three cycloalkyne-modules onto a platform compound bearing thiophene S,S-dioxide moiety and two azido groups. *Chem. Commun*. **2020**, *56*, 4720-3.

[5] Viault, G.; Dautrey, S.; Maindron, N.; Hardouin, J.; Renard, P-Y.; Romieu, A. The first "ready-to-use" benzene-based heterotrifunctional cross-linker for multiple bioconjugation. *Org. Biomol. Chem*. **2013**, *11*, 2693–705.

[6] Aucagne, V.; Leigh, D. A. Chemoselective formation of successive triazole linkages in one pot: "click-click" chemistry. *Org. Lett*. **2006**, *8*, 4505–7.

[7] Knall, A-C.; Hollauf, M.; Saf, R.; Slugovc, C. A trifunctional linker suitable for conducting three orthogonal click chemistries in one pot. *Org. Biomol. Chem.* **2016**, *14*, 10576-580.

[8] Tornøe, C. W.; Christensen, C.; Meldal, M. Peptidotriazoles on solid phase: [1,2,3]-triazoles by regiospecific copper(I)-catalyzed 1,3-dipolar cycloadditions of terminal alkynes to azides. *J. Org. Chem*. **2002**, *67*, 3057-64.

[9] Rostovtsev, V. V.; Green, L. G.; Fokin V. V.; Sharpless, K. B. A stepwise Huisgen cycloaddition process: copper(I)-catalyzed regioselective "ligation" of azides and terminal alkynes. *Angew. Chem., Int. Ed.* **2002**, *41*, 2596–9.

[10] Meldal, M. J.; Tornøe, C. W. Cu-catalyzed azide-alkyne cycloaddition. *Chem. Rev.* **2008**, *108*, 2952–3015.

[11] Wright, K.; Quinodoz, P.; Drouillat, B.; Couty, F. A one carbon staple for orthogonal copper-catalyzed azide–alkyne cycloadditions. *Chem. Commun*. **2017**, *53*, 321-3.

[12] Quinodoz, P.; Lo, C.; Kletskii, M. E.; Burov, O. N.; Marrot J.; Couty, F. Regio- and stereoselective synthesis of α-hydroxy-β-azido tetrazoles. *Org. Chem. Front.* **2015**, *2*, 492–6.

[13] Quinodoz, P.; Wright, K.; Drouillat, B.; Kletskii, M. E.; Burov, O. N.; Lisovin, A. V.; Couty, F. α-Hydroxy-tetrazoles as latent ethynyl moieties: a mechanistic investigation. *Eur. J. Org. Chem.* **2019**, 342–50.

[14] Fan, J.; Hu, M.; Zhan, P.; Peng, X. Energy transfer cassettes based on organic fluorophores: construction and applications in ratiometric sensing. *Chem. Soc. Rev*. **2013**, *42*, 29-43.

[15] Harriman, A. Artificial light-harvesting arrays for solar energy conversion. *Chem. Commun*., **2015**, *51*, 11745-56.

[16] Kozaki, M.; Suzuki, S.; Okada, K. Dendritic light-harvesting antennas with excitation energy gradients. *Chem. Lett.* **2013**, *42*, 1112-8.

[17] Gust, D.; Moore, T. A.; Moore, A. L. Solar fuels via artificial photosynthesis. *Acc. Chem. Res.* **2009**, *42*, 1890-8.

[18] Wasielewski, M. R. Self-assembly strategies for integrating light harvesting and charge separation in artificial photosynthetic systems. *Acc. Chem. Res.* **2009**, *42*, 1910-21.

[19] Ziessel, R.; Harriman, A. Artificial light-harvesting antennae: electronic energy transfer by way of molecular funnels. *Chem. Commun*. **2011**, *47*, 611-31.

[20] Ziessel, R.; Ulrich, G.; Haefele, A.; Harriman, A. An artificial light-harvesting array constructed from multiple BODIPY dyes. *J. Am. Chem. Soc*. **2013**, *135*, 11330−44.

[21] Odobel, F.; Pellegrin, Y.; Warnan, J. Bio-inspired artificial light-harvesting antennas for enhancement of solar energy capture in dye-sensitized solar cells. *Energy Environ. Sci.* **2013**, *6*, 2041-52.

[22] Charalambidis, G.; Karikis, K.; Georgilis, E.; Louahem M'Sabah, B.; Pellegrin, Y.; Planchat, A.; et al. Supramolecular architectures featuring the antenna effect in solid state DSSCs. *Sustainable Energy Fuels*. **2017**, *1*, 387-95.

[23] Wu, L.; Loudet, A.; Barhoumi, R.; Burghardt, R. C.; Burgess, K. Fluorescent cassettes for monitoring three-component interactions in vitro and in living cells. *J. Am. Chem. Soc*. **2009**, *131*, 9156–7.

[24] Shcherbakova, D. M.; Hint, M. A.; Joosen, L.; Gadella, T. W. J.; Verkusha, V. V. An orange fluorescent protein with a large Stokes shift for single-excitation multicolor FCCS and FRET imaging. *J. Am. Chem. Soc.* **2012**, *134*, 7913-23.

[25] Supramolecular Photochemistry: Controlling Photochemical Processes. Eds. V. Ramamurthy, V.; Y. Inoue, Y. New Jersey, John Wiley & Sons, **2011**, ISBN 978-0-470-23053-4.

[26] Cao, P.; Khorev, O.; Devaux, A.; Sägesser, L.; Kunzmann, A.; Ecker, A.; Häner, R.; Brühwiler, D.; Calzaferri, G.; Belser, P. Supramolecular Organization of Dye Molecules in Zeolite L Channels: Synthesis, Properties, and Composite Materials. *Chem. Eur. J.* **2016**, *22*, 4046-60.

[27] Gartzia-Rivero L.; Bañuelos J.; López-Arbeloa I. Photoactive Nanomaterials Inspired by Nature: LTL Zeolite Doped with Laser Dyes as Artificial Light Harvesting Systems. *Materials* **2017**, *10*, 495.

[28] Li, H.; Li, P. Luminescent materials of lanthanoid complexes hosted in zeolites. *Chem. Commun.* **2018**, *54*, 13884-93.

[29] Ulrich, G.; Ziessel, R.; Harriman, A. The chemistry of fluorescent BODIPY dyes: versatility unsurpassed. *Angew Chem Int Ed Engl*. **2008**, *47*, 1184-201.

[30] Bañuelos, J. BODIPY dye, the most versatile fluorophore ever. *Chem. Rec.* **2016**, *16*, 335-48.

[31] Prieto-Castañeda, A.; Avellanal-Zaballa, E.; Gartzia-Rivero, L.; Cerdán, L.; Agarrabeitia, A.; García-Moreno, I. et al Tailoring the Molecular Skeleton of Aza-BODIPYs to Design Photostable Red-Light-Emitting Laser Dyes. *ChemPhotoChem*. **2018**, *3*, 75-85.

[32] Feng, R.; Sato, N.; Yasuda, T.; Furuta, H.; Shimizu, S. Rational design of pyrrolopyrrole-aza-BODIPY-based acceptor–donor–acceptor triads for organic photovoltaics application. *Chem. Commun*., **2020**, *56*, 2975-78.

[33] Shi, Z.; Han, X.; Hu, W.; Bai, H.; Peng, B.; Ji, L.; Fan, Q.; Li, L.; Huang, W. Bioapplications of small molecule Aza-BODIPY: from rational structural design to in vivo investigations. *Chem. Soc. Rev*., **2020**, doi.org/10.1039/D0CS00234H

[34] Puntoriero, F.; Nastasi, F.; Campagna, S.; Bura, T.; Ziessel, R. Vectorial photoinduced energy transfer between boron dipyrromethene (BODIPY) chromophores across a fluorene bridge. *Chem. Eur. J.* **2010**, *16*, 8832-45.

[35] Hayashi, Y.; Yamaguchi, S.; Cha, W. Y.; Kim, D.; Shinokubo, H. Synthesis of directly connected BODIPY oligomers through Suzuki–Miyaura coupling. *Org. Lett.* **2011**, *13*, 2992-5.

[36] Nepomnyashchii, A. B.; Bröring, M.; Ahrens, J.; Bard, A. J. Synthesis, photophysical, electrochemical, and electrogenerated chemiluminescence studies. Multiple sequential electron transfers in BODIPY monomers, dimers, trimers, and polymer. *J. Am. Chem. Soc*. **2011**, *133*, 8633-45.

[37] Kaur, T.; Lakshmia, V. ; Ravikanth, M. Functionalized 3-pyrrolyl boron-dipyrromethenes. *RSC Adv*., **2013**, *3*, 2736-45.

[38] Duran-Sampedro, G.; Agarrabeitia, A. R.; Garcia-Moreno, I.; Gartzia-Rivero, L.; de la Moya, S.; Bañuelos, J.; et al. An asymmetric BODIPY triad with panchromatic absorption for high-performance red-edge laser emission. *Chem. Commun*. **2015**, *51*, 11382-5.

[39] Sharma, R.; Gobeze, H. B.; D'Souza, F.; Ravikanth, M. Panchromatic light capture and efficient excitation transfer leading to near-IR emission of BODIPY oligomers. *ChemPhysChem* **2016**, *17*, 2516-24.

[40] Diring, S.; Puntoriero, F.; Nastasi F.; Campagna S.; Ziessel, R. Star-shaped multichromophoric arrays from BODIPY dyes grafted on truxene core. *J. Am. Chem. Soc*. **2009**, *131*, 6108-10.

[41] Altan Bozdemir, O.; Cakmak, Y.; Sozmen, F.; Ozdemir, T.; Siemiarczuk, A.; Akkaya, E. U. Synthesis of symmetrical multichromophoric BODIPY dyes and their facile transformation into energy transfer cassettes. *Chem. Eur. J.* **2010**, *16*, 6346–51.

[42] Huaulmé, Q.; Cece, E.; Mirloup, A.; Ziessel, R. Star-shaped panchromatic absorbing dyes based on a triazatruxene platform with diketopyrrole and boron dipyrromethene substituents. *Tetrahedron Lett.* **2014**, *55*, 4953-8.

[43] Che, Y.; Yuan, X.; Cai, F.; Zhao, J.; Zhao, X.; Xu, H.; Liu, L. BODIPY−corrole dyad with truxene bridge: photophysical properties and application in triplet−triplet annihilation upconversion. *Dyes and Pigments*, **2019**, *171*, 107756.

[44] Mula, S.; Frein, S.; Russo, V.; Ulrich, G.; Ziessel, R.; Barberá, J.; Deschenaux, R. Red and blue liquid-crystalline borondipyrromethene dendrimers. *Chem. Mater*. **2015**, *27*, 2332-42.

[45] Thapaliya, E.R.; Zhang, Y.; Dhakal P.; Brown, A. S.; Wilson, J. N.; Collins, K.M.; Raymo, F. M. Bioimaging with macromolecular probes incorporating multiple BODIPY fluorophores. *Bioconjugate Chem*., **2017**, *28*, 1519-28.

[46] Bonaccorsi, P.; Aversa, M. C.; Barattucci, A.; Papalia, T.; Puntoriero, F.; Campagna, S. Artificial light-harvesting antenna systems grafted on a carbohydrate platform. *Chem. Commun.*, **2012**, *48*, 10550-2.

[47] Şenkuytu, E.; Eçik, E. T. New hexa-BODIPY functionalized dendrimeric cyclotriphosphazene conjugates as highly selective and sensitive fluorescent chemosensor for Co^{2+} ions. *Spectrochim. Acta A Mol. Biomol. Spectrosc.*, **2018**, *198*, 232-8.

[48] Bozdemir, O. A.; Erbas-Cakmak, S.; Ekiz, O. O.; Dana, A.; Akkaya, E. U. Towards unimolecular luminescent solar concentrators: BODIPY-based dendritic energy-transfer cascade with panchromatic absorption and monochromatized emission. *Angew. Chem. Int. Ed.* **2011**, *50*, 10907–12.

[49] Iehl, J.; Nierengarten, J.-F.; Harriman, A.; Bura, T.; Ziessel, R. Artificial light-harvesting arrays: electronic energy migration and trapping on a sphere and between spheres. *J. Am. Chem.Soc.* **2012**, *134*, 988–98.

[50] Yesilgul, N.; Seven, O.; Guliyev, R.; Akkaya, E. U. Energy harvesting in a BODIPY-functionalized rotaxane. *J. Org. Chem.* **2018**, *83*, 13228−32.

[51] Bura, T.; Nastasi, F.; Puntoriero, F.; Campagna, S.; Ziessel, R. Ultrafast energy transfer in triptycene-grafted BODIPY scaffoldings. *Chem. Eur. J*. **2013**, *19*, 8900–12.

[52] Emandi, G.; Browne, M. P.; Lyons, M. E.; Prior, C.; Senge, M. O. Triptycene scaffolds: Synthesis and properties of triptycene-derived Schiff base compounds for the selective and sensitive detection of CN^- and Cu^{2+}. *Tetrahedron*, **2017**, *73*, 2956-65.

[53] Emandi, G.; Shaker, Y. M.; Flanagan, K. J.; O'Brien, J. M.; Senge, M. O. Merging triptycene, BODIPY and porphyrin chemistry: Synthesis and properties of mono- and trisubstituted triptycene dye arrays. *Eur. J. Org. Chem.* **2017**, 6680-92.

[54] Sun, Y.; Sun, Y.; Zhao, S.; Cao, D.; Guan, R.; Z. Liu, Z.; et al. Efficient solution- and solid-state fluorescence for a series of 7-diethylaminocoumarin amide compounds. *Asian J. Org. Chem*. **2018**, *7*, 197-202.

[55] Mula, S.; Ray, A. K.; Banerjee, M.; Chaudhuri, T.; Dasgupta, K.; Chattopadhyay, S. Design and development of a new pyromethene dye with improved photostability and lasing efficiency: Theoretical rationalization of photophysical and photochemical properties. *J. Org. Chem.* **2008**, *73*, 2146-54.

[56] Lu, H.; Mack, J.; Yang, Y.; Shen, Z. Structural modification strategies for the rational design of red/NIR region BODIPYs. *Chem. Soc. Rev.* **2014**, *43*, 4778-823.

[57] Esnal, I.; Duran-Sampedro G.; Agarrabeitia A. R.; Bañuelos J.; García-Moreno I.; Macías M. A.; et al. Coumarin–BODIPY hybrids by heteroatom linkage: versatile, tunable and photostable dye lasers for UV irradiation. *Phys. Chem. Chem. Phys*. **2015**, *17*, 8239-47.

[58] He, L.; Zhu, S.; Liu, Y.; Xie, Y.; Xu, Q.; Wei, H.; Lin, W. Broadband light-harvesting molecular triads with high FRET efficiency based on the coumarin–rhodamine–BODIPY platform. *Chem. Eur. J.* **2015**, *21*, 12181-7.

[59] Zhao, Y.; Zhang, Y.; Lu, X.; Liu, Y.; Chen, M.; Wang, P.; et al. Through-bond energy transfer cassettes based on coumarin–BODIPY/distyryl BODIPY dyads with efficient energy efficiencies and large pseudo-Stokes' shifts. *J. Mater. Chem.* **2011**, *21*, 13168-71.

[60] Qian, Y.; Yang, B.; Shen, Y.; Du, Q.; Lin, L.; Lin, J.; Zhu, H. A BODIPY–coumarin-based selective fluorescent probe for rapidly detecting hydrogen sulfide in blood plasma and living cells. *Sens. Actuator, B* **2013**, *182*, 498-503.

[61] Zheng, K.; Chen, H.; Fang, S.; Wang, Y. A ratiometric fluorescent probe based on a BODIPY-Coumarin conjugate for sensing of nitroxyl in living cells. *Sens. Actuator, B* **2016**, *233*, 193-8.

[62] **CAUTION**: due to the high nitrogen atom content of **2**, hazards resulting from violent decomposition must be anticipated, though we have never observed such behaviour with these compounds.

[63] Wang, M.; Vicente, M. G. H.; Mason, D.; Bobadova-Parvanova, P. Stability of a series of BODIPYs in acidic conditions: an experimental and computational study into the role of the substituents at boron. *ACS Omega* **2018**, *3*, 5502−10.

[64] Baczko, K.; Fensterbank, H.; Berini, B.; Bordage, N.; Clavier, G.; Méallet-Renault, R.; et al. Azide-functionalized nanoparticles as quantized building block for the design of soft–soft fluorescent polystyrene core-PAMAM shell nanostructures. *J. Polym. Sci. Part A: Polym. Chem.* **2016**, *54*, 115-26.

[65] Chan, T. R.; Hilgraf R.; Sharpless, K. B.; Fokin V. V. Polytriazoles as copper(I)-stabilizing ligands in catalysis. *Org. Lett*. **2004**, *6*, 2853-5.

[66] Frisch, M. J.; Trucks, G. W.; Schlegel, H. B.; Scuseria, G. E.; Robb, M. A.; Cheeseman, J. R. et al. Gaussian 09, revision D.01; Gaussian Inc.: Wallingford, CT, 2013

[67] Chaudhuri, T.; Mula, S.; Chattopadhyay, S.; Banerjee, M. Photophysical properties of the 8-phenyl analogue of PM567: A theoretical rationalization. *Spectrochimica Acta Part A* **2010**, *75*, 739–744.

[68] Ostroverkhova, O. Organic optoelectronic materials: mechanisms and applications. *Chem. Rev*. **2016**, *116*, 13279-412.

[69] Taniguchi, M.; Du, H.; Lindsey, J. S. PhotochemCAD 3: Diverse modules for photophysical calculations with access to multiple spectral databases," *Photochem. Photobiol.* **2018**, *94*, 277–89.

[70] Fensterbank, H.; Baczko, K.; Constant, C.; Idttalbe, N.; Bourdreux, F.; Vallée, A.; et al. Sequential copper-catalyzed alkyne-azide cycloaddition and thiol-maleimide addition for the synthesis of photo- and/or electro-active fullerodendrimers and cysteine-functionalized fullerene derivatives. *J. Org. Chem.* **2016**, *81*, 8222-33.